Optimization of GCC Filler Use for Molded Pulp: A DOE Study of Pore Structure, Mechanical Properties, and Dewatering–Drying Efficiency

Jee-Hong Lee [a,*] Kyudeok Oh [b,c] Hye Jung Youn [b,c] and Hak Lae Lee [c]

Molded pulp packaging is rapidly growing as a sustainable packaging solution, but cost remains one of the biggest challenges. This study systematically investigates the potential use of mineral fillers as a cost-reduction strategy for molded pulp, using a design-of-experiments (DOE)-based approach. Laboratory-scale samples were produced with two ground calcium carbonate (GCC) fillers of different particle sizes at increasing dosages, and pore structure, mechanical properties, and dewatering/drying efficiency across stages of the molded-pulp process were assessed. With increasing filler dosage, mechanical properties decreased in three steps: slow initially, a steep mid-stage drop, then a slower final decline. The pore structure results correlated with this three-step change. The optimal filler-dosage range was determined from this three-step behavior and defined as the dosage corresponding to 80% of the maximum mechanical properties. GCC fillers improved the dewatering capability of the pulp suspension; however, this did not translate into improved dewatering efficiency at later stages. Future research is suggested to enable the successful application of mineral fillers in molded pulp products.

DOI: 10.15376/biores.21.1.2123-2175

Keywords: Molded pulp; Mineral fillers; Mechanical properties; Design of experiments (DOE); Optimal dosage; Cost reduction

*Contact information: a: Namyang R&D Center, Hyundai Motor Company, 150, Hyundaiyeonguso-ro, Namyang-eup, Hwaseong-si, Gyeonggi-do, 18280, Republic of Korea; b: Department of Agriculture, Forestry and Bioresources, College of Agriculture and Life Sciences, Seoul National University, 1 Gwanak-ro, Gwanak-gu, Seoul 08826, Korea; c: Research Institute of Agriculture and Life Sciences, College of Agriculture and Life Sciences, Seoul National University, 1 Gwanak-ro, Gwanak-gu, Seoul 08826, Korea; *Corresponding author: jhpechem@snu.ac.kr*

INTRODUCTION

Demand for sustainable packaging is accelerating, driven by regulatory restrictions on plastics, corporate sustainability commitments, and shifting consumer preferences toward environmentally responsible solutions (Diana *et al.* 2022; Herrmann *et al.* 2022; OECD 2022; McKinsey & Company 2025). Pulp- and paper-based packaging is one of the most preferred forms of sustainable packaging, capturing a notable share of the market and receiving strong consumer acceptance (Future Market Insights 2024; McKinsey & Company 2025).

Molded pulp is a fast-growing product category, showing continuous growth in both market size and scope of application (Zhang *et al.* 2022; Grand View Research 2024; IMFA 2025). The application scope of molded pulp has been progressively expanding, now encompassing food packaging, protective packaging for electronics and automotive

parts, horticultural trays and pots, beverage-bottle carriers, and single-use medical products (Zhang *et al.* 2022; IMFA 2025).

Economic feasibility remains one of the greatest challenges for sustainable packaging, and molded pulp is no exception (Byrne *et al.* 2023; De Canio 2023; McKinsey & Company 2025). Therefore, improving the cost efficiency of molded pulp is of great importance. Mineral fillers can reduce material costs by partially replacing the fiber component of the furnish, as they are generally less expensive than fibers (Amays *et al.* 2011; Cheng *et al.* 2011; Kang *et al.* 2020). Moreover, they can improve dewatering efficiency and reduce drying energy demand, owing to their lower water affinity and their role as "spacers" within the fiber network (Dong *et al.* 2008; Hubbe and Gill 2016). For these reasons, mineral fillers have been extensively used in printing and writing grades, and there has been a persistent trend toward higher filler use, up to 30% (Mahmud 2011; Hubbe and Gill 2016).

However, packaging grades such as kraft liner and corrugating medium generally avoid using mineral fillers because they deteriorate mechanical properties. Historically, molded pulp products were used predominantly for egg cartons and were made simply from recycled fibers and water (Wever and Twede 2007; Zhang *et al.* 2022; IMFA 2025). Over the past two decades, molded pulp has expanded beyond its traditional niches, with applications becoming increasingly diverse and materials correspondingly more varied (Debnath *et al.* 2022; Semple *et al.* 2022; Zhang *et al.* 2022). In these broad applications, not all may require extreme load-bearing strength.

In domains such as food-contact packaging and single-use medical products, once baseline mechanical performance is ensured, other characteristics—such as barrier and hygienic properties—may become more critical. In such cases, the incorporation of mineral fillers offers a viable route to cost reduction while maintaining the minimum mechanical durability required. Furthermore, with the increasing use of virgin pulp in molded pulp products for applications requiring hygienic standards or premium packaging quality, the substitution of a portion of pulp with mineral fillers is expected to yield greater cost-reduction benefits. Nevertheless, systematic investigations into the influence of mineral fillers on molded pulp products remain limited

Motivated by these considerations, the present study investigates the application potential of ground calcium carbonate (GCC) in molded pulp. Accordingly, the effects of GCC on coupled pore structure, mechanical performance, and dewatering/drying behavior were systematically quantified, and the filler dosage was optimized to minimize strength loss while maintaining sufficient filler content to achieve cost reduction. Laboratory-scale samples were prepared using a modified dynamic drainage jar (DDJ) for vacuum forming, followed by hot pressing.

A design of experiments (DOE) framework was applied to elucidate the effects of GCC particle size and dosage on (i) pore structure, (ii) mechanical properties (bending, burst, tear, tensile), and (iii) dewatering and drying efficiency. Data were analyzed using shared-intercept analysis of covariance (ANCOVA) and analysis of variance (ANOVA) with Dunnett's post hoc comparisons. Finally, polynomial models were fitted to characterize trends in mechanical properties and to identify optimal dosage regions that effectively increase filler loading while minimizing strength losses.

EXPERIMENTAL

Materials

Hardwood bleached kraft pulp (HwBKP) provided by Moorim P&P Co., Ltd. (Ulsan, Korea) was used as a pulp. Pulp suspension was prepared by disintegration according to TAPPI T205 (1995) (1.2 wt.%, 20,000 revolutions). Two types of ground calcium carbonates (GCCs) with different particle sizes were used: a coarse-grade sample (d_{10} = 0.604 μm, d_{50} = 2.135 μm, d_{90} = 8.052 μm, and a fine-grade sample (d_{10} = 0.328 μm, d_{50} = 0.798 μm, d_{90} = 1.423 μm, both measured using a Malvern Mastersizer 2000). A cationic polyacrylamide copolymer (Percol® 63, BASF, Ludwigshafen, Germany) was used as a retention aid.

Experimental Design

A design-of-experiments (DOE) approach was employed (Table 1). A two-factor, 2×3 factorial design was used with particle size (coarse vs. fine) and filler content (0, 10, 20%) as the primary factors. To better characterize the dose–response of mechanical properties, the coarse condition was augmented with two intermediate filler levels (5% and 15%), enabling regression modeling over a denser grid in the coarse region while preserving comparability at the common levels (0, 10, 20).

All samples were formulated to contain the same amount of oven-dry solids. Filler content was incorporated as a direct substitution for pulp. C-PAM was added at 0.1% of the total solids, equivalent to 1kg/t.

Table 1. Experimental Design

Content / Size	0%	5%	10%	15%	20%
Coarse	Control (Pulp 100%)	Pulp 95% and filler 5%	Pulp 90% and filler 10%	Pulp 85% and filler 15%	Pulp 80% and filler 20%
Fine	Control (Pulp 100%)	-	Pulp 90% and filler 10%	-	Pulp 80% and filler 20%

Note: The 0% coarse and 0% fine samples are identical (pulp 100%). C-PAM was included in all samples.

Molded Pulp Sample Preparation

Laboratory-scale molded pulp samples were prepared in two-steps: vacuum forming and hot-pressing.

Vacuum forming

Figure 1 illustrates the apparatus used for vacuum forming. The setup was modified from a dynamic drainage jar (DDJ; TAPPI T261 2000) by connecting a vacuum pump to the drainage line using a rubber tube (outer diameter 8 mm, inner diameter 5 mm). The cylindrical forming vessel had a diameter of 10.5 cm, and the drainage section was equipped with a #100 mesh screen (pore size 149 μm, ASTM E11 2022). A rubber packing ensured sealing between the cylinder and filtration flask.

Sample preparation was carried out by filling the vessel with pulp suspension and water to a total volume of 700 mL, with continuous stirring at 800 rpm. C-PAM was added and stirred for 30 s, followed by GCC addition and stirring for another 30 s, resulting in a suspension consistency of 0.51 wt%. Stirring was then stopped and the drain valve was

opened immediately, with vacuum drainage applied at 65 kPa. After completion of drainage, the vacuum was maintained for 30 s to ensure complete water removal

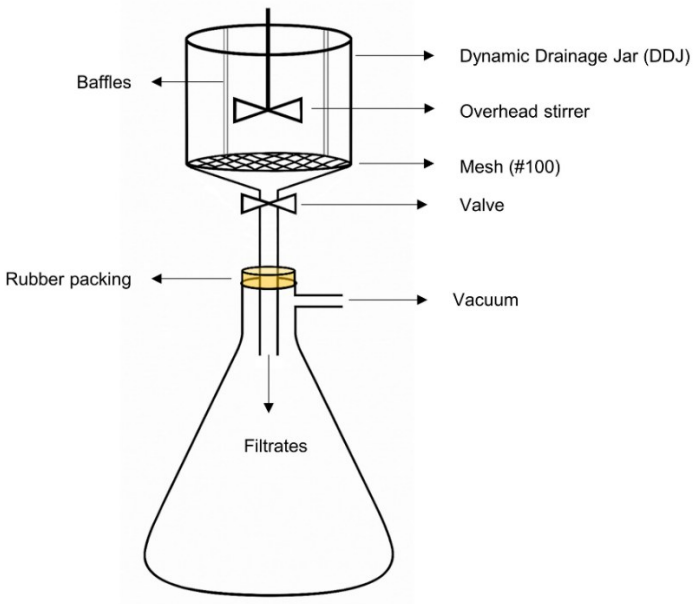

Fig. 1. Laboratory-scale apparatus used for vacuum forming, modified from a dynamic drainage jar (DDJ). This apparatus was designed to produce a flat circular specimen for laboratory-scale comparison, rather than a complex 3-dimensional geometry typically used for commercial molded pulp products.

Hot-pressing

Immediately after vacuum forming, the samples were subjected to hot-pressing. Non-stick aluminum foils were placed on the press surfaces, and the samples were positioned between them before pressing. Hot pressing was carried out at 110 °C and 2 MPa for 5 min. Following pressing, the samples were conditioned at 25 °C and 50% relative humidity under a pressure of 1.75 kg overnight.

Properties of Molded Pulp Samples

Ash content and pore structure

Ash content was measured according to TAPPI T211 (1993) in order to evaluate filler retention. The pore structure of molded pulp samples was assessed using calculated porosity and Gurley air resistance. Thickness was measured using a micrometer (L&W Micrometer 051, Lorentzen & Wettre, Sweden), and apparent density was calculated as grammage divided by thickness, in accordance with ISO 534 (2011). Gurley air resistance was determined following TAPPI T460 (1996). Porosity was determined from the apparent and true densities of the molded pulp samples (Eqs. 1 and 2),

$$\epsilon = 1 - \frac{\rho_{apparent}}{\rho_{true}} \quad (1)$$

$$\rho_{true} = \frac{w_{pulp} + w_{GCC}}{w_{pulp}/\rho_{pulp} + w_{GCC}/\rho_{GCC}} \quad (2)$$

where $\rho_{apparent}$ is the apparent density of molded pulp, ρ_{true} is the true density of molded pulp, w_{pulp} is the weight of pulp, ρ_{pulp} is 1.6 g/cm^3 (Daicho *et al.* 2019), w_{GCC} is the weight of GCC, and ρ_{GCC} is the 2.7 g/cm^3.

Mechanical properties

Four mechanical properties were assessed: bending (TAPPI T556 1995), burst (TAPPI T403 1997), tear (TAPPI T414 1998), and tensile (TAPPI T494 1996). All properties were expressed as mechanical indices, calculated as the measured strength divided by grammage, except for bending stiffness. This is because the grammage of molded pulp samples varied due to differences in filler retention, normalization by grammage was required. In the case of bending, however, stiffness depends strongly on the cube of thickness and on the elastic modulus of the material, and thus cannot be meaningfully normalized by grammage. Therefore, bending stiffness values were reported directly, as no standardized bending index exists.

Bending stiffness was determined with an L&W Bending Tester (L&W SE 160, Lorentzen & Wettre, Sweden). Burst strength was measured using a burst tester (KRK burst strength tester, Nerima, Tokyo, Japan), and the burst index was calculated. Tear resistance was measured with an Elmendorf tear tester (L&W SE 009, Lorentzen & Wettre, Sweden), and the tear index was calculated. Tensile strength was evaluated using a universal testing machine (Instron 5943, Instron Corp., Norwood, MA, USA), and the tensile index was determined

Dewatering and drying efficiency

The dewatering and drying efficiency was evaluated at different stages of the molded pulp process. At the stock preparation stage, Canadian Standard Freeness (CSF) was measured according to TAPPI T227 (1999) to characterize the drainage capacity of the suspension. At the forming and hot-pressing stages, solids content was determined using an infrared moisture analyzer (MS-70, A&D Company, Tokyo, Japan) for vacuum-formed samples and for samples subjected to 1 min of hot-pressing at 110 °C.

For both forming and hot-pressing stages, it was assumed that the sample temperature could not exceed 100 °C in the presence of water. In addition, for the hot-pressing stage, it was assumed that the sample already reached 100 °C after 1 min, such that the calculated drying energy reflected only the evaporation of water. Drying energy consumption and specific drying energy consumption (SEC) required to fully dry the samples were calculated according to Eqs. 3 and 4,

$$Q_{drying} = m_{water} \cdot \left(c_{water} \cdot \Delta T_{water} + L_{vapor}\right) + \sum_i m_i \cdot c_i \cdot \Delta T_i \quad (3)$$

$$SEC_{drying} = \frac{Q_{drying}}{w_{sample}} \quad (4)$$

where m_{water} is the mass of water to be evaporated (kg), c_{water} is the specific heat capacity of water (4.186 kJ·kg^{-1}·K^{-1}), ΔT_{water} is the temperature rise of water from the initial temperature (24 °C) to 100 °C, the maximum attainable temperature in the presence of liquid water, and L_{vapor} is the latent heat of vaporization of water (2257 kJ·kg^{-1}). The summation term $\Sigma m_i \cdot c_i \cdot \Delta T_i$ represents the total sensible heat required to raise the temperature of each solid component, where m_i is the mass (kg), c_i is the specific heat capacity (kJ·kg^{-1}·K^{-1}), and ΔT_i is the temperature rise (24 °C to 100 °C) of the i-th solid (pulp, GCC). Values of specific heat capacity used were c_{pulp} = 1.3 kJ·kg^{-1}·K^{-1} (Hatakeyama *et al.* 1982), and c_{GCC} = 0.9 kJ·kg^{-1}·K^{-1} (Roussel *et al.* 2005). Finally, w_{sample} is the oven-dry mass of the molded pulp sample (kg).

Statistical Analysis

Three complementary statistical approaches were used, each aligned with a specific question and data structure. First, because the coarse and fine GCC series contained different dosage levels (coarse: 0, 5, 10, 15, 20%; fine: 0, 10, 20%) while the 0% control specimen was identical for both sizes, the analysis was primarily base on a shared-intercept ANCOVA to quantify and compare the dose/ash–response slopes between particle sizes within a single model framework. Second, for responses that exhibited non-monotonic behavior with dosage (*i.e.*, not well represented by the first-order ANCOVA specification), the effects were evaluated of each formulation condition against the control (0%) using one-way ANOVA followed by Dunnett's post-hoc test, which controls the family-wise error rate for multiple comparisons to a common control. Finally, to characterize the non-linear mechanical reduction pattern with increasing filler and to identify an optimal dosage region, a polynomial regression was applied to the mechanical responses and a Monte Carlo–based weight-sensitivity analysis was performed of a composite mechanical index (a weighted summary of the measured mechanical properties), thereby assessing the robustness of the inferred optimum to application-dependent weighting choices. Assumptions for parametric inference were assessed using residual diagnostics (Q–Q plots, residuals *vs.* fitted, and scale-location plots) and formal tests (Shapiro–Wilk and Levene); diagnostic summaries and representative residual plots are provided in the Appendix/Supplementary Materials. Statistical significance was assessed at α=0.05.

Shared-intercept analysis of covariance (ANCOVA)

A shared-intercept ANCOVA model was used to evaluate (i) how filler dosage or ash content affected properties in both coarse and fine GCC, (ii) whether coarse and fine GCC differed in response, and (iii) whether these effects varied with ash content (Eq. 5). This model regresses the response on the covariate X, allowing slope differences between coarse and fine GCC while constraining the intercept to be common. Because the fine GCC data included only three dosage levels (0%, 10%, 20%), the ANCOVA was restricted to a first-order (straight-line) specification to enable direct slope comparisons between coarse and fine GCC. Note that ANCOVA itself is linear in parameters and can include higher-order terms; our analysis intentionally used a first-order form. Variables showing clear non-monotonic trends with dosage (*e.g.*, Gurley air resistance) were therefore not analyzed with this model. Prior to ANCOVA, assumptions were assessed as described above.

$$Y_{ij} = \mu + \gamma_c \cdot X_{ij} \cdot I(Size_i = Coarse) + \gamma_f \cdot X_{ij} \cdot I(Size_i = Fine) + \epsilon_{ij} \quad (5)$$

In Eq. 5, Y_{ij} is the response, μ is the shared intercept, X is the covariate of interest (either filler dosage or ash content), γ_c and γ_f is the slope coefficients for coarse and fine GCC, respectively, $I(\cdot)$ is an indicator function that equals 1 if the observation belongs to the specified group (coarse or fine GCC) and 0 otherwise, and ε_{ij} is the error term.

Based on hypothesis testing of slopes, the model evaluated (i) whether the covariate (either filler dosage or ash content) affected properties for coarse GCC (Eq. 6) and fine GCC (Eq. 7), and (ii) whether the two GCC types differed in response, which corresponds to the size × covariate interaction term (Eq. 8). Statistical significance was assessed at α = 0.05. Only summary ANCOVA results are presented in the manuscript; full model outputs and assumption checks are provided in the Appendix (Section A).

$$H_{0,1}: \gamma_c = 0 \quad (6)$$

$$H_{0,2}: \gamma_f = 0 \quad (7)$$

$$H_{0,3}: \gamma_c = \gamma_f \quad (8)$$

Analysis of variance (ANOVA) and post-hoc test

A one-way ANOVA was used to test for differences in the measured properties among groups. Prior to ANOVA, assumptions were assessed as described above. Two-sided Dunnett's post-hoc tests were then performed to compare each filler-added condition with the control, identifying which conditions differed significantly from the control. Only summary results are reported in the manuscript; full ANOVA tables, Dunnett comparisons, and assumption checks are provided in the Supplementary Materials (Section B).

Polynomial fitting of mechanical properties

Regression modeling was applied to coarse filler conditions (0, 5, 10, 15, and 20%) to analyze the trend of mechanical properties and to determine the optimal filler dosage point of molded pulp samples. All mechanical indices (bending, burst, tear, tensile) were normalized and integrated into composite mechanical index as a weighted average (Eqs. 9 and 10),

$$I_{norm}(x) = \frac{I(x)}{I(0)} \quad (9)$$

$$I_{Comp}(x) = w_{BS} \cdot BS_{norm}(x) + w_{BI} \cdot BI_{norm}(x) + w_{TeI} \cdot TeI_{norm}(x) + w_{TI} \cdot TI_{norm}(x)$$

$$(w_{BS} + w_{BI} + w_{TeI} + w_{TI} = 1) \quad (10)$$

where $I(x)$ is the mechanical index at a filler content of x%; $I(0)$ is the reference value obtained as the average of the measurements at 0% filler; $I_{norm}(x)$ is the normalized mechanical index at a given filler content; $I_{comp}(x)$ is composite mechanical index; The term $BS_{norm}(x)$, $BI_{norm}(x)$, $TeI_{norm}(x)$, and $TI_{norm}(x)$ represents bending stiffness, burst index, tear index, and tensile index, respectively. The weighting factors w_{BS}, w_{BI}, w_{TeI}, and w_{TI} correspond to the respective indices.

The relative importance of each mechanical property can vary depending on the target application and product design. Therefore, to analyze the sensitivity of the weighting, a Monte Carlo simulation was conducted to generate 1,000 sets of weights from a Dirichlet(1,1,1,1) distribution. For each simulated weighting scheme, polynomial fitting was applied. The polynomial model was chosen as the simplest model that satisfied the lack-of-fit (LOF) test, while model adequacy was also assessed using AICc and RMSE, and the model most frequently selected was adopted. Given that the experiment used five filler levels (0, 5, 10, 15, 20%), fitting was restricted to polynomial models; more complex nonlinear forms could not be estimated reliably from such limited design support.

Based on the qualitative analysis of the four-strength data and the cubic fitting result of the composite index, a region was identified where the rate of strength reduction increases sharply. This inflection point can be determined by locating where the second derivative of strength with respect to filler content, d^2(composite index)/d(filler)^2, equals zero. The optimal dosage point was defined as the point corresponding to 80% of the maximum reduction rate. This procedure was applied to each simulated weighting scheme, yielding the optimal filler dosage range. The fitted model was used exclusively for interpolation within the tested filler range and was not applied to extrapolation because of the limited degrees of freedom.

Software and implementation details

All analyses were performed in Python 3.13.5 using Jupyter Notebook with NumPy v2.1.3, SciPy v1.16.2, pandas v2.2.3, and statsmodels v0.14.5. Linear models (shared-intercept ANCOVA and one-way ANOVA) were fitted by ordinary least squares (OLS) using statsmodels. Shared-intercept ANCOVA was implemented by coding group-specific slope terms (X_C=X for Coarse and 0 otherwise; X_f=X for Fine and 0 otherwise) and fitting the models in Eq. 5. Slope hypotheses were evaluated using nested-model F-test (statsmodels f_test) at $\alpha=0.05$. Following one-way ANOVA, Dunnett's post-hoc comparisons versus the 0% control were performed as two-sided tests using scipy.stats.dunnett reporting adjusted p-values and simultaneous confidence intervals. Normality and homoscedasticity diagnostics were performed on OLS residuals using Shapiro–Wilk (scipy.stats.shapiro) and Levene tests (scipy.stats.levene, center=median). Monte Carlo weight-sensitivity analysis used 1,000 Dirichlet(1,1,1,1) weight vectors (seed = 1234) generated with NumPy; polynomial models (degrees 1–3) were fitted by OLS using NumPy least squares. Model adequacy was evaluated using a pure-error lack-of-fit F-test by partitioning the residual sum of squares into pure error (from replicates at identical predictor levels) and lack-of-fit; and testing $F=MS_{LoF}/MS_{pure}$; p-values were computed from the F distribution (scipy.stats.f)

RESULTS AND DISCUSSION

Ash Content and Pore Structure

Figure 2a and 2b present the results for the ash content of molded pulp samples. The hypothesis test (H_0: $\gamma_c = \gamma_f$, $p < 0.001$) indicated that filler retention differed significantly depending on the particle size of the GCC. Ash content increased linearly with dosage for both GCC types. The slopes of the predicted regression lines showed that 61.5% of the dosed fine GCC was retained ($\gamma_f = 0.615$) whereas 78% of the dosed coarse GCC was retained ($\gamma_c = 0.780$). The higher retention of coarse GCC can be attributed to its larger particle size, leading to greater entrapment in the fiber network.

The hypothesis test (H_0: $\gamma_c=0$, H_0: $\gamma_f=0$, $p < 0.001$) indicated that the addition of both coarse and fine GCC increased the porosity (Fig. 2c and 2d). According to Dunnett's post-hoc test, porosity did not significantly change at low dosages (5% and 10%), whereas it increased at higher dosages (15% and 20%). The influence of filler addition on the pore structure of the fiber network can be attributed to two competing effects: pore filling and structural interference (Hubbe and Gill 2016). Fillers can occupy the inter-fiber voids, thereby densifying the network and reducing porosity. Conversely, fillers may disrupt fiber-fiber bonding by occupying bonding sites, leading to a less compact and bulkier structure that increases porosity. At low filler levels, these two effects counterbalance each other, resulting in nearly unchanged porosity. However, at higher filler levels, the disruptive effect on the fiber network becomes dominant due to limited packing efficiency and extensive bonding interference, which ultimately leads to increased porosity.

The same principle can be applied to the Gurley air resistance results (Fig. 2e), where increased resistance was observed at low dosages (5% and 10%), as confirmed by Dunnett's post-hoc test. The air permeability in paper can be described by Darcy's law and the Kozeny–Carman equation (Knauf and Doshi 1986; Shallhorn and Gurnagul 2009), which indicate that air permeability in the fiber network is governed by structural factors such as porosity, pore size distribution, tortuosity, and specific surface area.

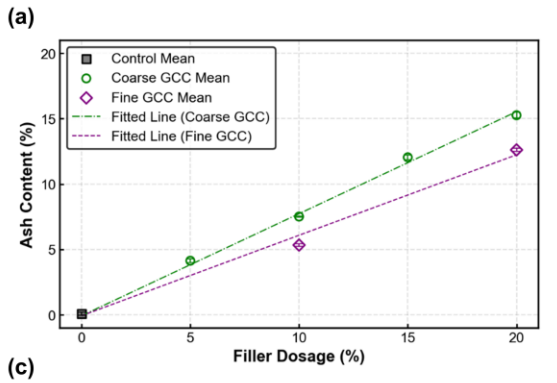

(b)

α=0.05

Filler Dosage (%) vs Ash Content (%)			
H_0	γ (estimate)	p	Significance
$\gamma_c = 0$	$\gamma_c = 0.780$	<0.001	Significant
$\gamma_f = 0$	$\gamma_f = 0.615$	<0.001	Significant
$\gamma_c = \gamma_f$	$\gamma_c - \gamma_f = 0.165$	<0.001	Significant

Levene's test rejected homogeneity of variance ($p < 0.001$). However, residual diagnostics (Q–Q and residuals vs fitted) showed no severe departures, so the model was retained and results were interpreted with this limitation noted..

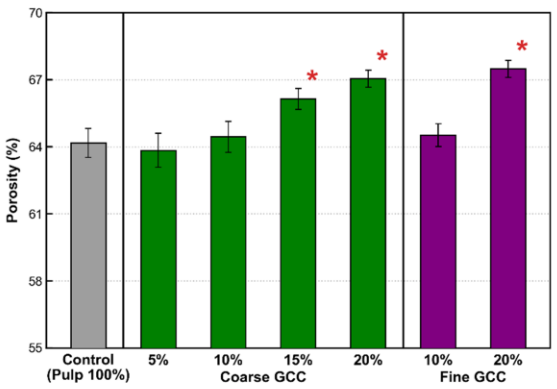

(d)

α=0.05

Filler Dosage (%) vs Porosity (%)			
H_0	γ (estimate)	p	Significance
$\gamma_c = 0$	$\gamma_c = 0.175$	<0.001	Significant
$\gamma_f = 0$	$\gamma_f = 0.191$	<0.001	Significant
$\gamma_c = \gamma_f$	$\gamma_c - \gamma_f = -0.016$	0.470	Not significant
Ash Content (%) vs Porosity (%)			
H_0	γ (estimate)	p	Significance
$\gamma_c = 0$	$\gamma_c = 0.224$	<0.001	Significant
$\gamma_f = 0$	$\gamma_f = 0.313$	<0.001	Significant
$\gamma_c = \gamma_f$	$\gamma_c - \gamma_f = -0.089$	0.009	Significant

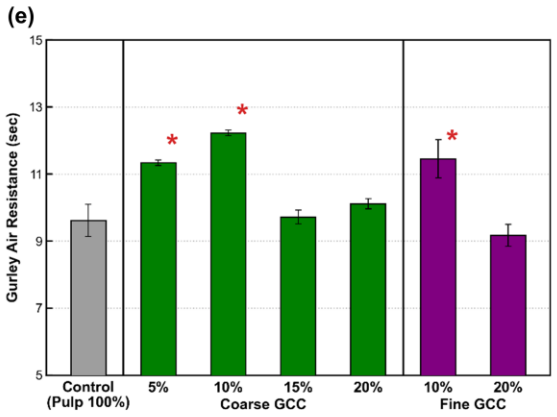

Fig. 2. Ash content and pore structure of molded pulp samples. (a) Ash content with ANCOVA-fitted line, (b) ANCOVA summary for ash content, (c) Porosity as a function of filler dosage, (d) ANCOVA summary for porosity with respect to filler dosage and ash content, (e) Gurley air resistance versus filler dosage. Red asterisks indicate groups significantly different from controls according to Dunnett's post hoc test. Because Gurley air resistance exhibited a non-monotonic trend, ANCOVA was not applied. Complete tables and assumption checks (Shapiro–Wilk, Levene) are provided in the Supplementary Material (ANCOVA: Sections A.1–A.2; ANOVA: Section B.1–B.2).

At low filler levels, both pore filling and structural interference occur simultaneously. The unchanged porosity suggests that these two effects largely offset each other (Fig. 2c); however, the increase in Gurley resistance indicates that the pore structure was nevertheless substantially modified. Pore filling may have reduced the average pore size and increased both the specific surface area and tortuosity, explaining the observed rise in air-flow resistance. At higher filler levels, by contrast, the influence of structural interference becomes more pronounced, leading to increased porosity and a looser network structure, which facilitates air flow and thereby lowers the Gurley resistance.

(a)

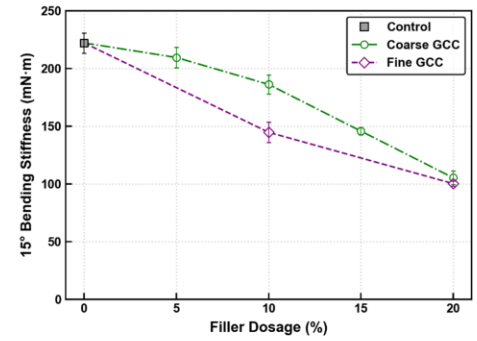

(b)

α=0.05

Filler Dosage (%) vs 15° Bending Stiffness (mN·m)			
H_0	γ (estimate)	p	Significance
$\gamma_c = 0$	γ_c = -5.632	<0.001	Significant
$\gamma_f = 0$	γ_f = -6.807	<0.001	Significant
$\gamma_c = \gamma_f$	$\gamma_c - \gamma_f$ = 1.175	0.002	Significant
Ash Content (%) vs 15° Bending Stiffness (mN·m)			
H_0	γ (estimate)	p	Significance
$\gamma_c = 0$	γ_c = -6.995	<0.001	Significant
$\gamma_f = 0$	γ_f = -10.730	<0.001	Significant
$\gamma_c = \gamma_f$	$\gamma_c - \gamma_f$ = 3.735	<0.001	Significant

Levene's test for the ANCOVA residuals showed borderline evidence against homogeneity of variances (p = 0.0497); residual diagnostics did not show severe patterns, so results were interpreted with this limitation noted.

(c)

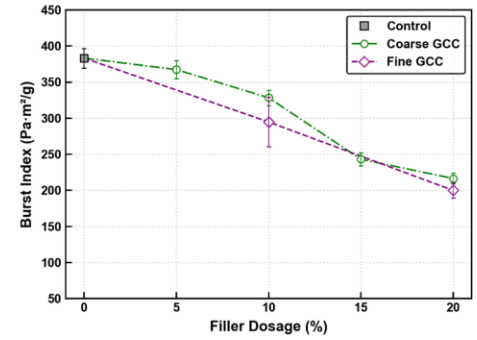

(d)

α=0.05

Filler Dosage (%) vs Burst Index (Pa·m²/g)			
H_0	γ (estimate)	p	Significance
$\gamma_c = 0$	γ_c = -9.088	<0.001	Significant
$\gamma_f = 0$	γ_f = -10.000	<0.001	Significant
$\gamma_c = \gamma_f$	$\gamma_c - \gamma_f$ = 0.912	0.126	Not significant
Ash Content (%) vs Burst Index (Pa·m²/g)			
H_0	γ (estimate)	p	Significance
$\gamma_c = 0$	γ_c = -11.49	<0.001	Significant
$\gamma_f = 0$	γ_f = -16.02	<0.001	Significant
$\gamma_c = \gamma_f$	$\gamma_c - \gamma_f$ = 4.53	<0.001	Significant

(e)

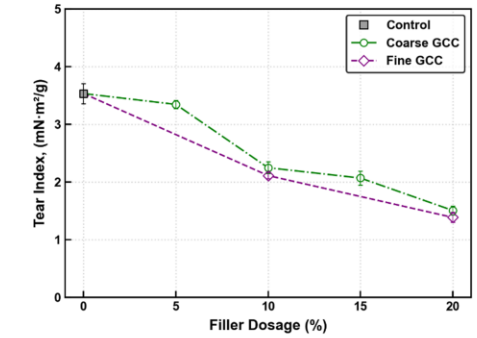

(f)

α=0.05

Filler Dosage (%) vs Tear Index (mN·m²/g)			
H_0	γ (estimate)	p	Significance
$\gamma_c = 0$	γ_c = -0.101	<0.001	Significant
$\gamma_f = 0$	γ_f = -0.114	<0.001	Significant
$\gamma_c = \gamma_f$	$\gamma_c - \gamma_f$ = 0.013	0.046	Significant
Ash Content (%) vs Tear Index (mN·m²/g)			
H_0	γ (estimate)	p	Significance
$\gamma_c = 0$	γ_c = -0.125	<0.001	Significant
$\gamma_f = 0$	γ_f = -0.179	<0.001	Significant
$\gamma_c = \gamma_f$	$\gamma_c - \gamma_f$ = 0.054	<0.001	Significant

(g)

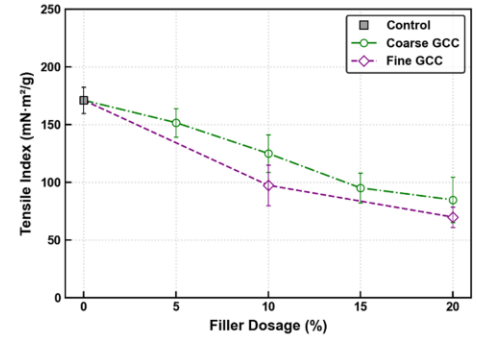

(h)

α=0.05

Filler Dosage (%) vs Tensile Index (mN·m²/g)			
H_0	γ (estimate)	p	Significance
$\gamma_c = 0$	γ_c = -4.251	<0.001	Significant
$\gamma_f = 0$	γ_f = -5.239	<0.001	Significant
$\gamma_c = \gamma_f$	$\gamma_c - \gamma_f$ = 0.988	0.040	Significant
Ash Content (%) vs Tensile Index (mN·m²/g)			
H_0	γ (estimate)	p	Significance
$\gamma_c = 0$	γ_c = -5.283	<0.001	Significant
$\gamma_f = 0$	γ_f = -8.233	<0.001	Significant
$\gamma_c = \gamma_f$	$\gamma_c - \gamma_f$ = 2.95	<0.001	Significant

Fig. 3. Mechanical properties of molded pulp samples. (a) 15° bending stiffness as a function of filler dosage, (b) ANCOVA summary of bending stiffness with respect to filler dosage and ash content, (c) burst index vs filler dosage, (d) ANCOVA summary of burst index with respect to filler dosage and ash content, (e) tear index vs filler dosage, (f) ANCOVA summary of tear index with respect to filler dosage and ash content, (g) tensile index vs filler dosage, and (h) ANCOVA summary of tensile index with respect to filler dosage and ash content. Complete ANCOVA tables and assumption checks (Shapiro–Wilk, Levene) are provided in the Appendix (Sections A.3–A.6).

Another interesting observation was that the gradients of coarse and fine GCCs were not significantly different when porosity was plotted against filler dosage (H_0: $\gamma_c = \gamma_f$, $p = 0.470$). However, when porosity was plotted against ash content, the gradients differed significantly (H_0: $\gamma_c = \gamma_f$, $p = 0.009$), indicating that fine GCC produced greater interference in the fiber network at comparable ash levels. This is consistent with prior reports that finer particles interfere more with fiber–fiber bonding, thereby loosening the network (Chauhan *et al.* 2013; Hubbe and Gill 2016).

Mechanical Properties

Figure 3 presents the results for four different mechanical properties of molded pulp samples. Both coarse and fine GCC led to significant decreases in these properties (H_0: $\gamma_c = 0$, H_0: $\gamma_f = 0$, $p < 0.001$). Although burst index versus filler dosage was an exception (H_0: $\gamma_c = \gamma_f$, $p = 0.126$), the hypothesis test indicated that mechanical properties overall differed significantly, depending on the particle size of the GCC, with the effect being more pronounced when properties were plotted against ash content (max $p = 0.046$, min $p < 0.001$). Fine GCC exhibited a steeper gradient, which was likely due to their higher tendency to adsorb onto fiber surfaces and thereby interfering more strongly with fiber–fiber bonding.

For coarse GCC, the reduction extent of all mechanical properties was relatively slow at low dosages (5 to 10%), followed by a pronounced decline at mid-to-high dosages (10 to 15%). At the highest dosage range (15 to 20%), the decline continued but became less steep for burst, tear, and tensile indices, while bending stiffness showed a similar trend. This pattern can be attributed to the structural changes described previously. At low dosage, structural interference is limited because the pore-filling effect counteracts the bonding interference caused by the filler, resulting in only minor reductions in mechanical properties. As the dosage increases, structural interference becomes more pronounced, leading to a sharp decline. At high dosage, however, much of the fiber–fiber bonding had already been disrupted, so further additions exerted only a limited incremental effect, producing a slower but continued decline in mechanical properties.

Fine GCC exhibited a steeper decline at 0 to 10% filler dosage than at 10 to 20% (Fig. 3), with the exception of burst index, despite little change in bulk porosity (Fig. 2c). This observation shows that the high propensity of fine particles to weaken fiber–fiber bonding results in a sharp reduction even at low-to-mid dosages. At 20%, the bonding capacity of the fiber network is already largely compromised, so additional filler produces only a limited incremental effect, resulting in a slower reduction rate.

Regression modeling of the composite mechanical index corroborated the trend of mechanical properties with respect to filler dosage (Fig. 4). Based on 1,000 weight combinations (w_{BS}, w_{BI}, w_{TeI}, w_{TI}) generated by Monte Carlo sampling from a Dirichlet(1,1,1,1) distribution, the coarse GCC composite mechanical index was predominantly cubic (86.5% of cases; fixed random seed = 1234). This indicates that, overall, the mechanical properties of molded pulp samples decline slowly at low dosages, reach their maximum rate of reduction at mid dosages, and then decrease more gradually again at high dosages. The filler dosage corresponding to the maximum rate of reduction, based on the range of model values across different weight combinations, was 9.5 to 15.7%. At this point, the mechanical properties of the molded pulp samples decreased by 22 to 37% from the original level ($I_{comp} = 0.63$ to 0.78). The optimal filler dosage range, defined as the dosage that reaches 80% of this maximum reduction rate, was 4.5 to 8.7%, within which the mechanical properties decreased by 8 to 14% ($I_{comp} = 0.86$ to 0.92). These results

suggest that fillers can be added at a median dosage of 6.6%, with only a modest reduction in mechanical properties (11% at the median).

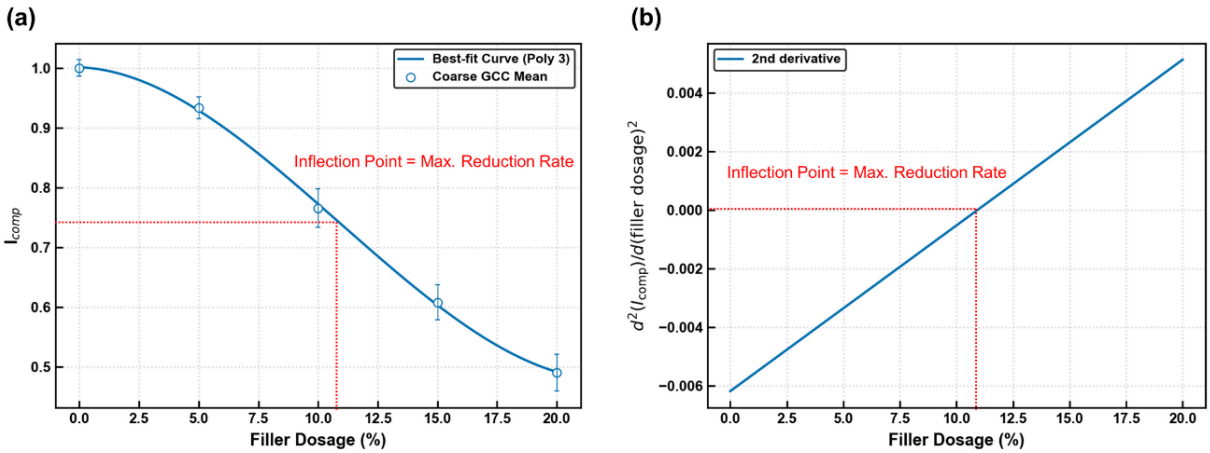

(c)

Filler Dosage at Max. Reduction Rate (%)	I_{comp} at Max. Reduction Rate	Filler Dosage at 80% of Max. Reduction Rate	I_{comp} at 80% of Max. Reduction Rate
9.5 – 15.7	0.63 – 0.78	4.5 – 8.7	0.86 – 0.92

Fig. 4. Representative curves showing the composite mechanical index and the filler dosage ranges corresponding to the maximum and 80% of the maximum reduction rates. (a) Best-fit curve when all weights are equal (w_{BS} = w_{BI} = w_{Tel} = w_{TI} = 0.25). (b) Second derivative of the curve in (a). (c) Summary of filler dosage and the composite mechanical indices (I_{comp}) at the maximum and 80% reduction rates. The filler dosage at the maximum reduction rate corresponds to the point where the second derivative equals zero (red dotted lines in panels (a) and (b)).

Dewatering and Drying Efficiency

Figures 5 and 6 present the dewatering and drying performance of molded pulp samples at each processing step. As shown in Fig. 5a and b, CSF increased significantly with filler dosage (H_0: $\gamma_c = 0$, H_0: $\gamma_f = 0$, $p < 0.001$). When plotted against filler dosage, no significant difference was observed between coarse and fine GCC (H_0: $\gamma_c = \gamma_f$, $p = 0.141$). However, when plotted against ash content, a significant difference emerged (H_0: $\gamma_c = \gamma_f$, $p = 0.002$), indicating that the lower retention of fine GCC reduced its effectiveness in improving drainage.

Figures 5c to g show the total drying energy required after forming and after one minute of hot-pressing. At both stages, samples with increasing GCC required less total drying energy (H_0: $\gamma_c = 0$, H_0: $\gamma_f = 0$, $p < 0.001$). However, the corresponding SEC results (Fig. 6) do not support an improvement in drying efficiency. Instead, the reduced energy demand is consistent with a smaller amount of water to be evaporated—likely due to lower solids retention—rather than enhanced heat or mass transfer. SEC after forming (Fig. 6a, c and e) was not significantly influenced by fillers, whether plotted against filler dosage or retained ash (H_0: $\gamma_c = 0$, H_0: $\gamma_f = 0$, $p = 0.053$ to 0.904). After one minute of hot-pressing, SEC decreased slightly (~2.1 to 2.8% in most cases, except fine GCC at 20%), but the effect showed no dose-dependence and close to the significance threshold (Fig. 6b, d, and f), providing only weak evidence for filler-induced improvements in drying efficiency.

(a)

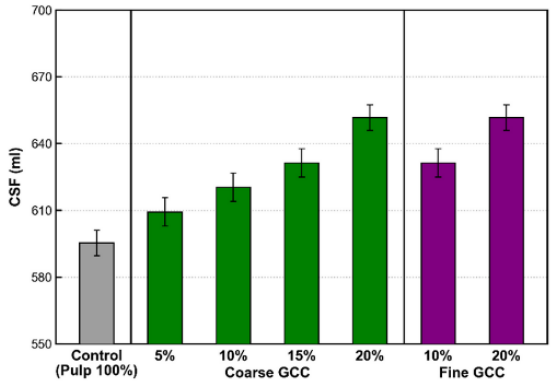

(b)

α=0.05

Filler Dosage (%) vs CSF (ml)			
H_0	γ (estimate)	p	Significance
$\gamma_c = 0$	$\gamma_c = 2.577$	<0.001	Significant
$\gamma_f = 0$	$\gamma_f = 2.908$	<0.001	Significant
$\gamma_c = \gamma_f$	$\gamma_c - \gamma_f = -0.311$	0.141	Not significant
Ash Content (%) vs CSF (ml)			
H_0	γ (estimate)	p	Significance
$\gamma_c = 0$	$\gamma_c = 3.207$	<0.001	Significant
$\gamma_f = 0$	$\gamma_f = 4.590$	<0.001	Significant
$\gamma_c = \gamma_f$	$\gamma_c - \gamma_f = -1.383$	0.002	Significant

(c)

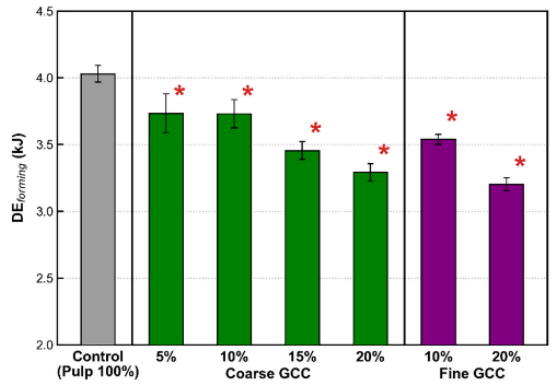

(d)

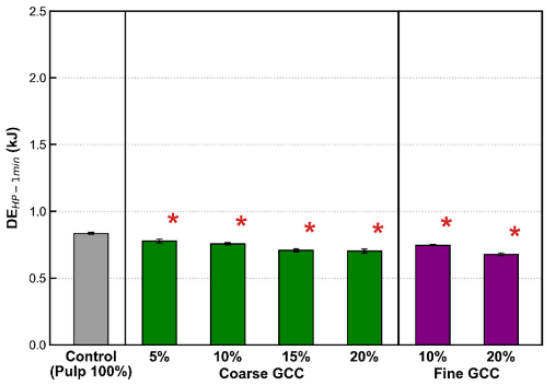

(e)

% Reduction in $DE_{forming}$ (vs control)					
Coarse				Fine	
5%	10%	15%	20%	10%	20%
-7.4	-7.4	-14.3	-18.3	-12.2	-20.5

(f)

% Reduction in $DE_{HP-1min}$ (vs control)					
Coarse				Fine	
5%	10%	15%	20%	10%	20%
-6.9	-9.4	-15.2	-15.9	-10.5	-18.8

(g)

α=0.05

Filler Dosage (%) vs $DE_{forming}$ (kJ)			
H_0	γ (estimate)	p	Significance
$\gamma_c = 0$	$\gamma_c = -0.034$	<0.001	Significant
$\gamma_f = 0$	$\gamma_f = -0.040$	<0.001	Significant
$\gamma_c = \gamma_f$	$\gamma_c - \gamma_f = 0.006$	0.067	Not significant
Ash Content (%) vs $DE_{forming}$ (kJ)			
H_0	γ (estimate)	p	Significance
$\gamma_c = 0$	$\gamma_c = -0.043$	<0.001	Significant
$\gamma_f = 0$	$\gamma_f = -0.064$	<0.001	Significant
$\gamma_c = \gamma_f$	$\gamma_c - \gamma_f = 0.021$	<0.001	Significant

(h)

α=0.05

Filler Dosage (%) vs $DE_{HP-1min}$ (kJ)			
H_0	γ (estimate)	p	Significance
$\gamma_c = 0$	$\gamma_c = -0.007$	<0.001	Significant
$\gamma_f = 0$	$\gamma_f = -0.007$	<0.001	Significant
$\gamma_c = \gamma_f$	$\gamma_c - \gamma_f = 0.001$	0.252	Not significant
Ash Content (%) vs $DE_{HP-1min}$ (kJ)			
H_0	γ (estimate)	p	Significance
$\gamma_c = 0$	$\gamma_c = -0.008$	<0.001	Significant
$\gamma_f = 0$	$\gamma_f = -0.012$	<0.001	Significant
$\gamma_c = \gamma_f$	$\gamma_c - \gamma_f = 0.003$	<0.001	Significant

Fig. 5. Canadian Standard Freeness (CSF) and drying energy required to fully dry molded pulp samples at each processing step. (a) CSF of the suspension. (b) ANCOVA summary for CSF. (c) Drying energy required after forming ($DE_{forming}$). (d) Drying energy required after one minute of hot-pressing ($DE_{HP-1min}$). (e) Percentage reduction in $DE_{forming}$ relative to the control. (f) Percentage reduction in $DE_{HP-1min}$ relative to the control. (g) ANCOVA summary for $DE_{forming}$. (h) ANCOVA summary for $DE_{HP-1min}$. Red asterisks in panels (c) and (d) denote groups significantly different from the control according to Dunnett's post-hoc test ($p < 0.050$). Dunnett comparisons are not shown for (a) because Shapiro–Wilk rejected normality for CSF ($p < 0.001$). Complete tables and assumption checks (Shapiro–Wilk, Levene) are provided in the Appendix (ANCOVA: Sections A.7–A.9; ANOVA: Section B.3–B.5).

(a)

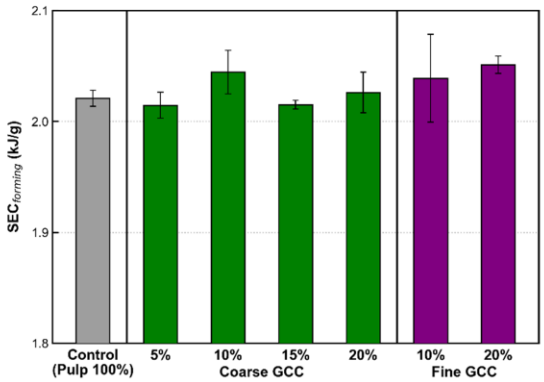

(b)

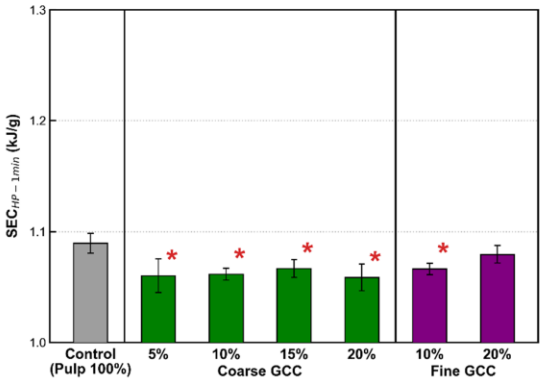

(c)

% Reduction in $SEC_{forming}$ (vs Control)						
Control	Coarse				Fine	
-	5%	10%	15%	20%	10%	20%
-	-0.3	1.2	-0.3	0.3	0.9	1.5
Solids Content (%) after Forming						
22.4	22.6	21.4	22.6	22.1	21.6	21.1

(d)

% Reduction in $SEC_{forming}$ (vs Control)						
Control	Coarse				Fine	
-	5%	10%	15%	20%	10%	20%
-	-2.7	-2.6	-2.1	-2.8	-2.1	-0.9
Solids Content (%) after Forming						
51.7	53.0	53.0	52.7	53.1	52.8	52.2

(e)

α=0.05

Filler Dosage (%) vs $SEC_{forming}$ (kJ/g)			
H_0	γ (estimate)	p	Significance
$\gamma_c = 0$	$\gamma_c = 1.801 \times 10^{-4}$	0.797	Not significant
$\gamma_f = 0$	$\gamma_f = 0.001$	0.053	Not significant
$\gamma_c = \gamma_f$	$\gamma_c - \gamma_f = -0.001$	0.065	Not significant
Ash Content (%) vs $SEC_{forming}$(kJ/g)			
H_0	γ (estimate)	p-value	Significance
$\gamma_c = 0$	$\gamma_c = 1.083 \times 10^{-4}$	0.904	Not significant
$\gamma_f = 0$	$\gamma_f = 0.002$	0.062	Not significant
$\gamma_c = \gamma_f$	$\gamma_c - \gamma_f = -0.002$	0.042	Significant

Shapiro–Wilk tests indicated departures from normality for both the filler-dosage and ash-content model (p = 0.049 and 0.034, respectively). However, residual diagnostics suggested only mild tail deviations and no major heteroscedasticity; therefore, the models were retained and interpreted with this limitation noted.

(f)

α=0.05

Filler Dosage (%) vs $SEC_{HP-1min}$ (kJ/g)			
H_0	γ (estimate)	p	Significance
$\gamma_c = 0$	$\gamma_c = -9.157 \times 10^{-4}$	0.046	Significant
$\gamma_f = 0$	$\gamma_f = -2.753 \times 10^{-5}$	0.951	Not significant
$\gamma_c = \gamma_f$	$\gamma_c - \gamma_f = -8.882 \times 10^{-4}$	0.042	Significant
Ash Content (%) vs $SEC_{HP-1min}$ (kJ/g)			
H_0	γ (estimate)	p	Significance
$\gamma_c = 0$	$\gamma_c = -0.001$	0.050*	Significant
$\gamma_f = 0$	$\gamma_f = 3.541 \times 10^{-5}$	0.960	Not significant
$\gamma_c = \gamma_f$	$\gamma_c - \gamma_f = -0.001$	0.068	Not significant

*exact p = 0.04975

Fig. 6. Specific energy consumption required to fully dry molded pulp samples at each processing step. (a) Specific energy consumption after forming ($SEC_{forming}$). (b) Specific energy consumption after one minute of hot-pressing ($SEC_{HP-1\ min}$). (c) Percentage reduction in $SEC_{forming}$ relative to the control, and solids content after forming. (d) Percentage reduction in $SEC_{HP-1\ min}$ relative to the control, and solids content after one minute of hot-pressing. (e) ANCOVA summary for $SEC_{forming}$. (f) ANCOVA summary for $SEC_{HP-1\ min}$. Red asterisks in panels (a) and (b) denote groups significantly different from the control according to Dunnett's post-hoc test ($p < 0.05$). SEC responses showed weak dependence on dose/ash content relative to specimen-to-specimen scatter ($R^2 \leq 0.27$; Appendix A.10–A.11). Accordingly, ANCOVA slope estimates were used primarily for hypothesis testing ($\gamma = 0$, $\gamma_c = \gamma_f$), supported by residual diagnostics reported in the Appendix. Complete tables and assumption checks (Shapiro–Wilk, Levene) are provided in the Appendix (ANCOVA: Sections A.10–A.11; ANOVA: Section B.6–B.7).

In papermaking, fillers are well known to improve solids content after pressing, thereby enhancing dewatering (Chauhan *et al.* 2011; Hua *et al.* 2011; Sutman 2011; Lee *et al.* 2021). Previous studies reported that a 10% increase in ash content raises post-press solids by approximately 0.8 to 2.6% (Hua *et al.* 2011; Sutman 2011; Lee *et al.* 2021). Since a 1% increase in post-press solids is expected to reduce steam consumption by ~4%, this improvement translates directly into thermal energy savings (Mohey 2016). Mineral fillers are generally believed to reduce water affinity and act as spacers that open transport pathways within the fiber network (Dong *et al.* 2008; Hubbe and Gill 2016). Although

reports on molded pulp are scarce, one recent study using a thermoforming process found that increasing GCC or kaolin shortened the required vacuum suction times, whereas adding talc or kaolin raised post-press solids by 0.6 to 1.5% per 10% filler (Gaskin *et al.* 2024). In the present study, the CSF results (Fig. 5a) likewise suggest that GCC enhanced drainage, and pore structure analysis (Fig. 2) indicates that fillers acted as spacers that altered the fiber network toward a bulkier structure, particularly at higher dosages (15 to 20%).

Nevertheless, SEC results provide little evidence that GCC improved overall dewatering or drying efficiency. Given that the filler effect on post-press solids is typically small (≤2.6% per 10% increase in ash content, according to previous studies (Hua *et al.* 2011; Sutman 2011; Lee *et al.* 2021; Gaskin *et al.* 2024), its contribution may have been masked by the processing conditions used here. The vacuum forming condition (65 kPa, maintained 30 s after audible drainage ceased) likely removed most of the free water from inter-fiber voids, equalizing the residual water content across all filler dosages. During hot-pressing, pressing and heating act simultaneously, combining capillary drainage with heat-driven diffusion and evaporation. Under such conditions—where pressing and thermal effects occur simultaneously—their combined action makes it difficult to isolate the specific contribution of fillers to capillary drainage. These findings imply that the dewatering benefits of fillers are strongly contingent on the processing sequence and conditions, including the criteria for ending suction forming and the subsequent pressing and drying strategy.

Limitations and Future Works

This study demonstrated the potential of mineral fillers as a cost-reduction strategy in molded pulp. As an initial step, the investigation was confined to the effects of filler particle size and dosage. However, the optimal dosage may shift when strength-enhancing additives (*e.g.*, dry strength agents) are used with fillers—an interaction not evaluated here. The influence of processing parameters (*e.g.*, hot-press pressure and temperature) was also not considered, even though these factors can modify the fiber network and, consequently, mechanical performance. Within the conditions tested in this study, fillers did not measurably improve dewatering or drying efficiency; accordingly, our results support only the cost savings from the directly replacing fiber with lower-cost filler. Future work should pair fillers with strength additives, map the influence of forming/pressing/drying conditions—including dewatering and energy use—and validate the findings at pilot or industrial scale. In addition, fillers may also contribute to other properties required for molded-pulp packaging—such as optical, surface/printability, and barrier performance—which were outside our scope and should be assessed in future studies.

CONCLUSIONS

1. The mechanical properties of molded pulp exhibited a three-step reduction pattern with increasing filler dosage: a gradual decrease at low dosage (5 to 10%), a sharp decline at mid-to-high dosage (10 to 15%), and a slower decline at higher dosage (15 to 20%). This three-step reduction can be explained by structural changes in the molded pulp due to ground calcium carbonate (GCC) addition, as supported by the pore-structure results.

2. Based on the three-step reduction pattern, the optimal filler dosage range was defined as the level corresponding to 80% of the maximum mechanical property reduction. The results showed that GCC fillers can be added at 6.6% (the median of the optimal range), with only a modest reduction in mechanical properties (11% at the median).
3. The Canadian standard freeness (CSF) results showed that the addition of GCC fillers improved the drainage of the pulp suspension; however, this improvement did not translate into enhanced dewatering efficiency after suction forming or 1 min of hot pressing, which was likely due to the influence of the processing conditions.

ACKNOWLEDGMENTS

Conflict of Interest

This work is unrelated to Hyundai Motor Company; the Hyundai Motor Company–affiliated author conducted the research independently and in a personal capacity. All authors declare that they have no known competing financial interests or personal relationships that could have appeared to influence the work reported in this paper.

REFERENCES CITED

Amays, J. J., Doelle, K., and Mahmud, S. (2011). "A comparative study of different fillers on uncoated eucalyptus digital printing paper properties: A pilot scale approach," in: *TAPPI PaperCon Conference*, Covington, KY, USA.

ASTM E11-22 (2022). "Standard specification for woven wire test sieve cloth and test sieves," ASTM International, West Conshohocken, PA, USA.

Byrne, C., Pley, C., Schorscher, P., Brandon, Z., Gatumbu, P., Mallinson, C., and Vaghela, M. (2023). "A mixed-methods analysis of the climate impact, acceptability, feasibility and cost of switching from single-use pulp to reusable plastic trays in a large NHS trust," *Future Healthcare Journal* 10(2), 157-160. https://doi.org/10.7861/fhj.2022-0129

Chauhan, V. S., Bhardwaj, N. K., and Chakrabarti, S. K. (2013). "Effect of particle size of magnesium silicate filler on physical properties of paper," *The Canadian Journal of Chemical Engineering* 91(5), 855-861. https://doi.org/10.1002/cjce.21708

Chauhan, V. S., Sharma, A., Chakrabarti, S. K., and Varadhan, R. (2011). "Energy savings through increased filler loading in paper," *IPPTA: Quarterly Journal of Indian Pulp and Paper Technical Association* 23(3), 171-176.

Cheng, W., Broadus, K., and Ancona, M. (2011). "New technology for increased filler use and fiber savings in graphic grades," in: *TAPPI PaperCon Conference*, Covington, KY, USA, pp. 616-620.

Daicho, K., Kobayashi, K., Fujisawa, S., and Saito, T. (2019). "Crystallinity-independent yet modification-dependent true density of nanocellulose," *Biomacromolecules* 21(2), 939-945. https://doi.org/10.1021/acs.biomac.9b01584

De Canio, F. (2023). "Consumer willingness to pay more for pro-environmental packages: The moderating role of familiarity," *Journal of Environmental Management* 339, 117828. https://doi.org/10.1016/j.jenvman.2023.117828

Debnath, M., Sarder, M., Pal, L., and Hubbe, M. (2022). "Molded pulp products for

sustainable packaging: Production rate challenges and product opportunities," *BioResources* 17(1), 17-54. https://doi.org/10.15376/biores.17.2.Debnath

Diana, Z., Reilly, K., Karasik, R., Vegh, T., Wang, Y., Wong, Z., Dunn, L., Blasiak, R., Dunphy-Daly, M., Rittschof, D., Vermeer, D., Pickle, A., and Virdin, J. (2022). "Voluntary commitments made by the world's largest companies focus on recycling and packaging over other actions to address the plastics crisis," *One Earth* 5(11), 1286-1306. https://doi.org/10.1016/j.oneear.2022.10.008

Dong, C., Song, D., Patterson, T., Ragauskas, A., and Deng, Y. (2008). "Energy saving in papermaking through filler addition," *Industrial & Engineering Chemistry Research* 47(21), 8430-8435. https://doi.org/10.1021/ie8011159

Future Market Insights (2024). "Sustainable packaging market: Sustainable packaging market size, share & forecast 2025 to 2035," (https://www.futuremarketinsights.com/reports/sustainable-packaging-market).

Gaskin, E., Reed, G., Preston, J., and Biza, P. (2024). "The use of minerals in fiber-based packaging and pulp molding," *TAPPI Journal* 23(1), 25-32. https://doi.org/10.32964/tj23.1.25

Grand View Research. (2024). "Molded fiber packaging market (2025–2030)," (https://www.grandviewresearch.com/industry-analysis/molded-fiber-packaging-market-report).

Hatakeyama, T., Nakamura, K., and Hatakeyama, H. (1982). "Studies on heat capacity of cellulose and lignin by differential scanning calorimetry," *Polymer* 23(12), 1801-1804.

Herrmann, C., Rhein, S., and Sträter, K. F. (2022). "Consumers' sustainability-related perception of and willingness-to-pay for food packaging alternatives," *Resources, Conservation and Recycling* 181, article 106219. https://doi.org/10.1016/j.resconrec.2022.106219

Hua, X., Owston, T., and Laleg, M. (2011). "Wet-web strength and pressability of highly-filled sheets," in: *TAPPI PaperCon Conference*, Covington, KY, USA.

Hubbe, M. A., and Gill, R. A. (2016). "Fillers for papermaking: A review of their properties, usage practices, and their mechanistic role," *BioResources* 11(1), 2886-2963. https://doi.org/10.15376/biores.11.1.2886-2963

International Molded Fiber Association (IMFA) (2025). "Molded fiber 101 / Masterclass," (https://imfa.org), Accessed October 3, 2025.

ISO 534 (2011). "Paper and board—Determination of thickness, density, and specific volume," International Organization for Standardization, Geneva, Switzerland.

Kang, D. S., Han, J. S., Choi, J. S., and Seo, Y. B. (2020). "Development of deformable calcium carbonate for high filler paper," *ACS Omega* 5(25), 15202-15209. https://doi.org/10.1021/acsomega.0c01179

Knauf, G. H., and Doshi, M. R. (1986). "Calculations of aerodynamic porosity, specific surface area, and specific volume from Gurley seconds measurements," *IPC Technical Paper Series* 183, 1-8.

Lee, M. W., Jung, S. Y., and Seo, Y. B. (2021). "Energy saving in papermaking by application of hybrid calcium carbonate," *BioResources* 16(3), 5011-5023. https://doi.org/10.15376/biores.16.3.5011-5023

Mahmud, S. (2011). "A comparative study of different fillers on uncoated digital printing paper," in: *TAPPI PaperCon Conference*, Covington, KY, USA.

McKinsey & Company (2025). "Sustainability in packaging 2025: Inside the minds of global consumers," (https://www.mckinsey.com/industries/packaging-and-paper/our-

insights/sustainability-in-packaging-2025-inside-the-minds-of-global-consumers).
Mohey, G. (2016). *Energy efficiency opportunities in a pulp drying machine*, Master's Thesis, University of Gävle, Gävle, Sweden.
OECD (2022). "Global plastics outlook: Economic drivers, environmental impacts and policy options," (https://doi.org/10.1787/de747aef-en).
Roussel, M., Guy, A., Shaw, L., and Cara, J. (2005). "The use of calcium carbonate in polyolefins offers significant improvement in productivity," *Target* 300, article 350.
Semple, K. E., Zhou, C., Rojas, O. J., Nguegang Nkeuwa, W., and Dai, C. (2022). "Moulded pulp fibers for disposable food packaging: A state-of-the-art review," *Food Packaging and Shelf Life* 33, article 100908. https://doi.org/10.1016/j.fpsl.2022.100908
Shallhorn, P., and Gurnagul, N. (2009). "A simple model of the air permeability of paper," in *Advances in Pulp and Paper Research: Transactions of the 14th Fundamental Research Symposium*, S. J. I'Anson (Ed.), FRC, pp. 475-490. https://doi.org/10.15376/frc.2009.1.475
Sutman, F. J. (2011). "The influence of filler content and process additives on wet web strength and runnability," in: *TAPPI PaperCon Conference*, Covington, KY, USA, pp. 919-925.
TAPPI T 205 sp-95 (1995). "Forming handsheets for physical tests of pulp," TAPPI Press, Atlanta, GA, USA.
TAPPI T 211 om-93 (1993). "Ash in wood, pulp, paper, and paperboard: Combustion at 525°C," TAPPI Press, Atlanta, GA, USA.
TAPPI T 227 om-99 (1999). "Freeness of pulp (Canadian standard method)," TAPPI Press, Atlanta, GA, USA.
TAPPI T 261 cm-00 (2000). "Fines fraction of paper stock by wet screening," TAPPI Press, Atlanta, GA, USA.
TAPPI T 403 om-97 (1997). "Bursting strength of paper," TAPPI Press, Atlanta, GA, USA.
TAPPI T 414 om-98 (1998). "Internal tearing resistance of paper (Elmendorf-type method)," TAPPI Press, Atlanta, GA, USA.
TAPPI T 460 om-96 (1996). "Air resistance of paper (Gurley method)," TAPPI Press, Atlanta, GA, USA.
TAPPI T 494 om-96 (1996). "Tensile properties of paper and paperboard (using constant rate of elongation apparatus)," TAPPI Press, Atlanta, GA, USA.
TAPPI T 556 pm-95 (1995). "Bending resistance of paper and paperboard (Taber-type tester in basic configuration)," TAPPI Press, Atlanta, GA, USA.
Wever, R., and Twede, D. (2007). "The history of molded fiber packaging: A 20th-century pulp story," in *Proceedings of the 23rd IAPRI Symposium on Packaging*, Pira International, Windsor, UK, 1-8.
Zhang, Y., Duan, C., Bokka, S. K., He, Z., and Ni, Y. (2022). "Molded fiber and pulp products as green and sustainable alternatives to plastics: A mini review," *Journal of Bioresources and Bioproducts* 7(1), 14-25. https://doi.org/10.1016/j.jobab.2021.10.003

Article submitted: October 19, 2025; Peer review competed: November 1, 2025; Revised version received: December 19, 2025; Accepted: December 29, 2025; Published: January 21, 2026.
DOI: 10.15376/biores.21.1.2123-2175

APPENDIX

Assumption checks were performed on the OLS residuals, and Levene's test was conducted using median centering. Independence was ensured by the experimental design through the use of separately prepared replicate specimens at each condition. Multicollinearity was not a practical concern for the models used: in the shared-intercept ANCOVA, the group-specific slope regressors are mutually exclusive by construction; and in polynomial regression, polynomial bases can be correlated, but individual coefficients were not interpreted, and model adequacy/selection was evaluated using lack-of-fit testing and fit criteria.

ANCOVA Results

1. Ash Content

Levene's test rejected homogeneity of variance. However, residual diagnostics showed no severe departures, so the model was retained, and results were interpreted with this limitation noted.

1.1. ANCOVA fitted line

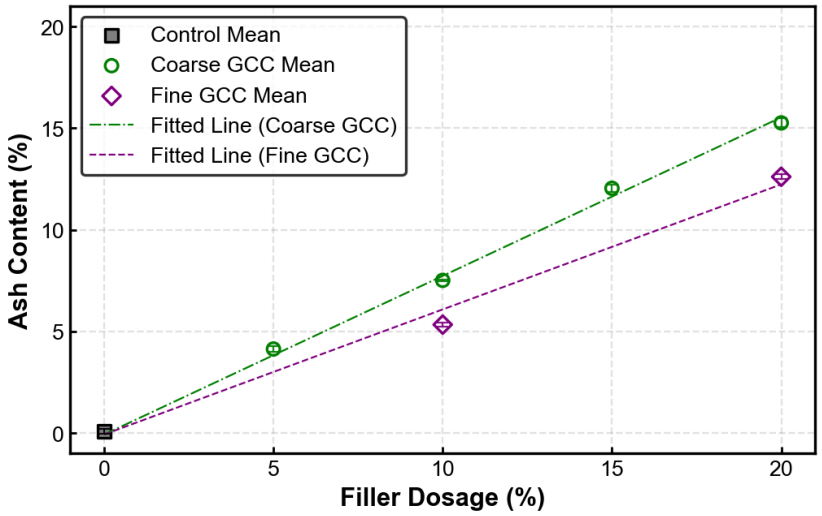

1.2. ANCOVA Slope estimates and 95% CI

Parameter	Estimate	95% CI (lower)	95% CI (upper)
γ_c	0.780	0.747	0.813
γ_f	0.615	0.581	0.649
$\gamma_c - \gamma_f$	0.165	0.133	0.196

1.3. ANCOVA hypothesis test table

H_0	F	df	p	Result
$\gamma_c = 0$	2449.16	18	<0.001	Significant
$\gamma_f = 0$	1440.29	18	<0.001	Significant
$\gamma_c = \gamma_f$	121.02	18	<0.001	Significant

1.4. ANCOVA fit summary

n	df_resid	R^2
21	18	0.993

1.5. ANCOVA assumption check

Test	Statistic	p	Result
Shapiro-Wilk	0.93	0.172	Not significant (normality not rejected)
Levene's test	14.91	<0.001	Significant (equal variances rejected)

1.6. Representative residual plots (Q-Q plot, residuals vs. fitted)

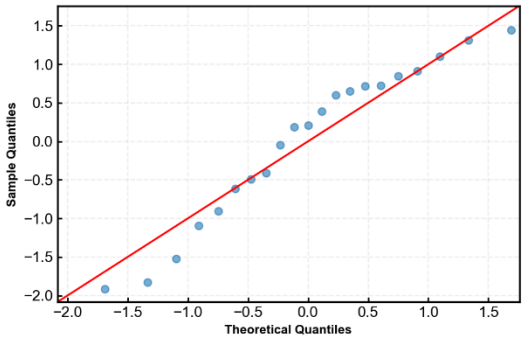

2. Porosity

2-1. vs Filler Dosage

2-1.1. ANCOVA fitted line

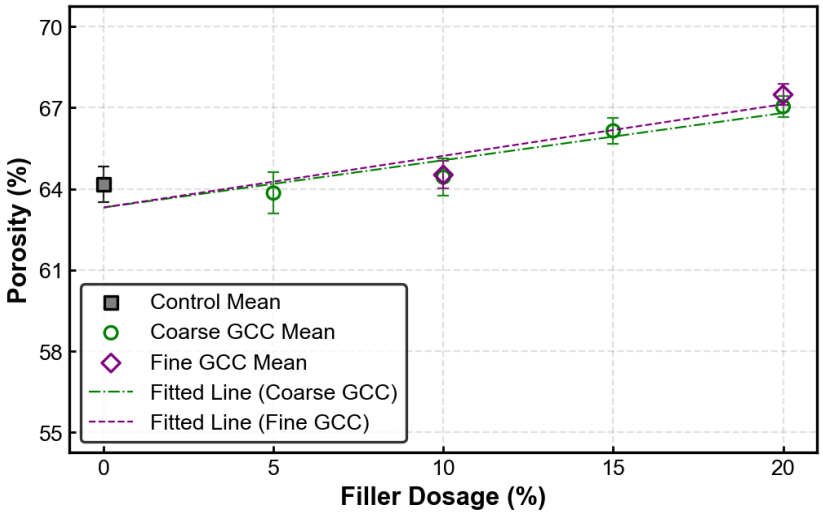

2-1.2. ANCOVA Slope estimates and 95% CI

Parameter	Estimate	95% CI (lower)	95% CI (upper)
γ_c	0.175	0.127	0.223
γ_f	0.191	0.142	0.240
$\gamma_c - \gamma_f$	-0.016	-0.062	0.029

2-1.3. ANCOVA hypothesis test table

H_0	F	df	p	Result
$\gamma_c = 0$	56.27	25	<0.001	Significant
$\gamma_f = 0$	63.56	25	<0.001	Significant
$\gamma_c = \gamma_f$	0.54	25	0.470	Not Significant

2-1.4. ANCOVA fit summary

n	df_resid	R^2
28	25	0.755

2-1.5. ANCOVA assumption check

Test	Statistic	p	Result
Shapiro-Wilk	0.97	0.597	Not significant (normality not rejected)
Levene's test	0.04	0.960	Not significant (equal variances not rejected)

2-1.6. Representative residual plots (Q-Q plot, residuals vs. fitted)

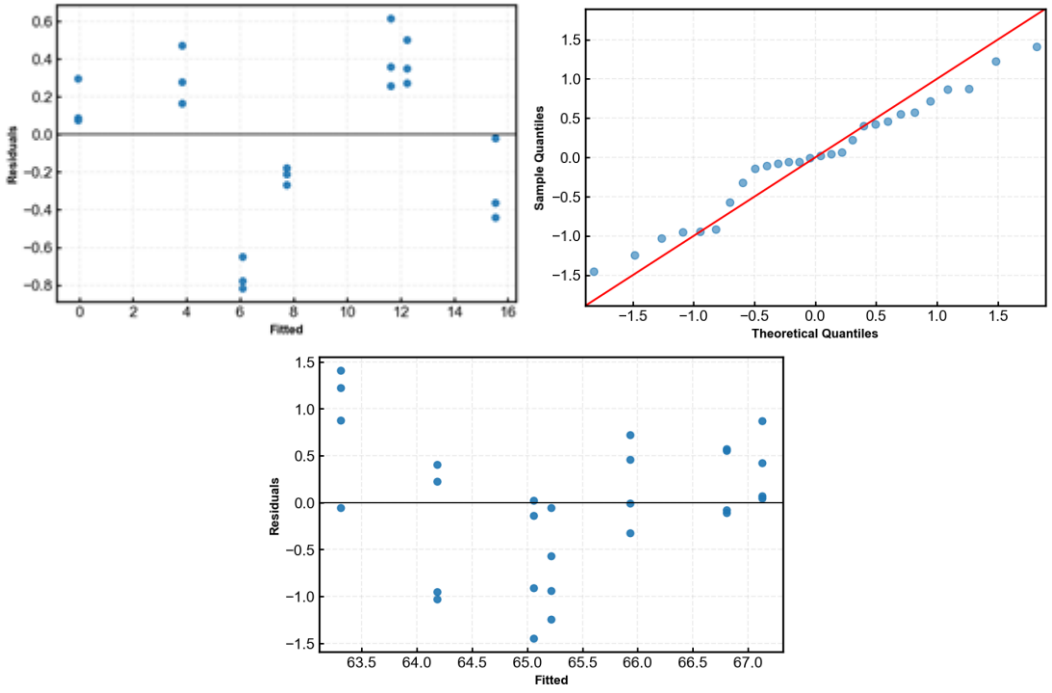

2-2. vs Ash Content

2-2.1. ANCOVA fitted line

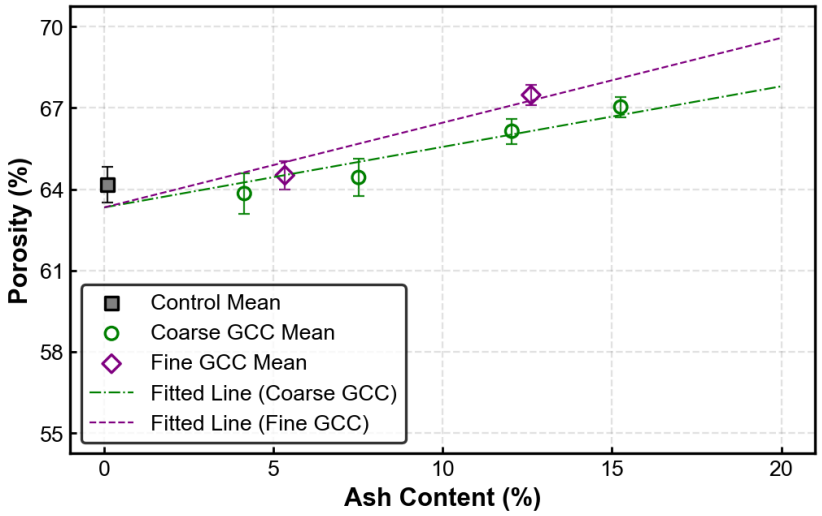

2-2.2. ANCOVA Slope estimates and 95% CI

Parameter	Estimate	95% CI (lower)	95% CI (upper)
γ_c	0.223	0.165	0.282
γ_f	0.313	0.238	0.388
$\gamma_c - \gamma_f$	-0.089	-0.154	-0.024

2-2.3. ANCOVA hypothesis test table

H_0	F	df	p	Result
$\gamma_c = 0$	62.65	25	<0.001	Significant
$\gamma_f = 0$	73.99	25	<0.001	Significant
$\gamma_c = \gamma_f$	8.02	25	0.009	Significant

2-2.4. ANCOVA fit summary

n	df_resid	R^2
28	25	0.780

2-2.5. ANCOVA assumption check

Test	Statistic	p	Result
Shapiro-Wilk	0.97	0.688	Not significant (normality not rejected)
Levene's test	0.10	0.902	Not significant (equal variances not rejected)

2-1.6. Representative residual plots (Q-Q plot, residuals vs fitted)

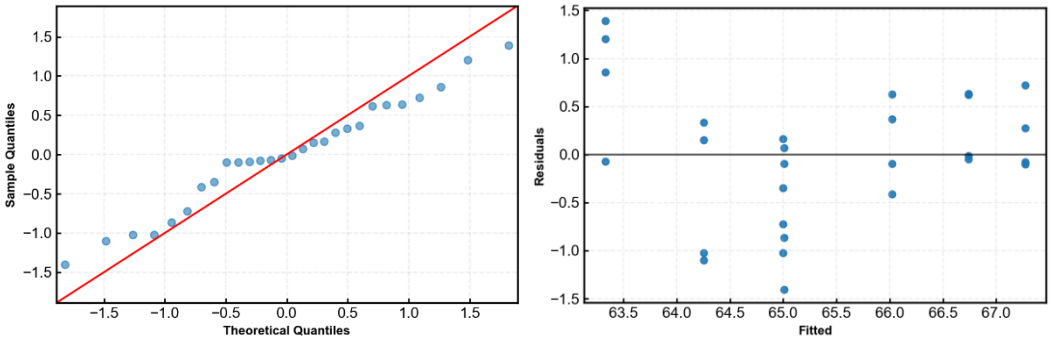

3. 15° Bending Stiffness

Levene's test showed borderline evidence against homogeneity of variances. However, residual diagnostics did not show severe patterns, so results were interpreted with this limitation noted.

3-1. vs Filler Dosage

3-1.1. ANCOVA fitted line

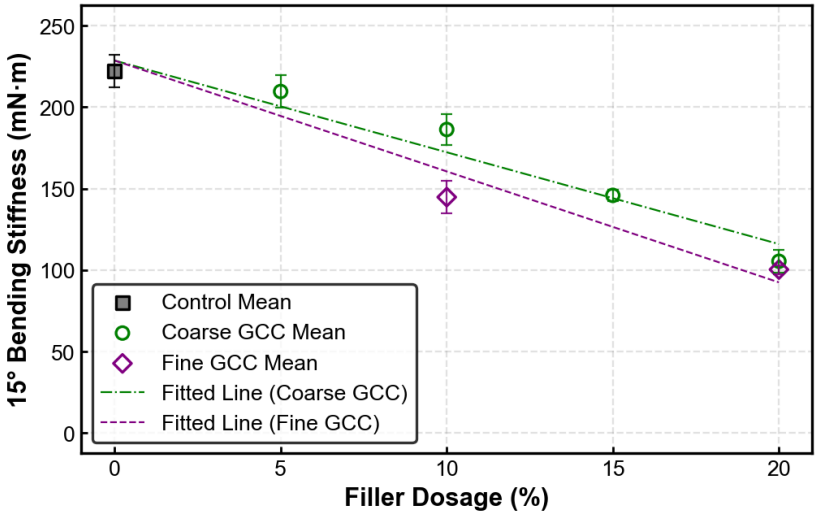

3-1.2. ANCOVA Slope estimates and 95% CI

Parameter	Estimate	95% CI (lower)	95% CI (upper)
γ_c	-5.632	-6.363	-4.901
γ_f	-6.807	-7.559	-6.055
γ_c - γ_f	1.175	0.480	1.871

3-1.3. ANCOVA hypothesis test table

H_0	F	df	p	Result
$\gamma_c = 0$	246.09	32	<0.001	Significant
$\gamma_f = 0$	339.92	32	<0.001	Significant
$\gamma_c = \gamma_f$	11.86	32	0.002	Significant

2-1.4. ANCOVA fit summary

n	df_resid	R^2
35	32	0.923

3-1.5. ANCOVA assumption check

Test	Statistic	p	Result
Shapiro-Wilk	0.97	0.560	Not significant (normality not rejected)
Levene's test	0.88	0.425	Not significant (equal variances not rejected)

3-1.6. Representative residual plots (Q-Q plot, residuals vs fitted)

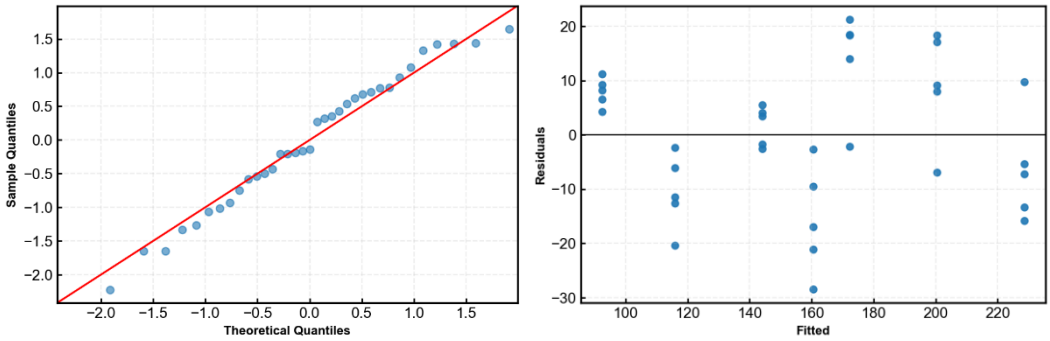

3-2. vs Ash Content

3-2.1. ANCOVA fitted line

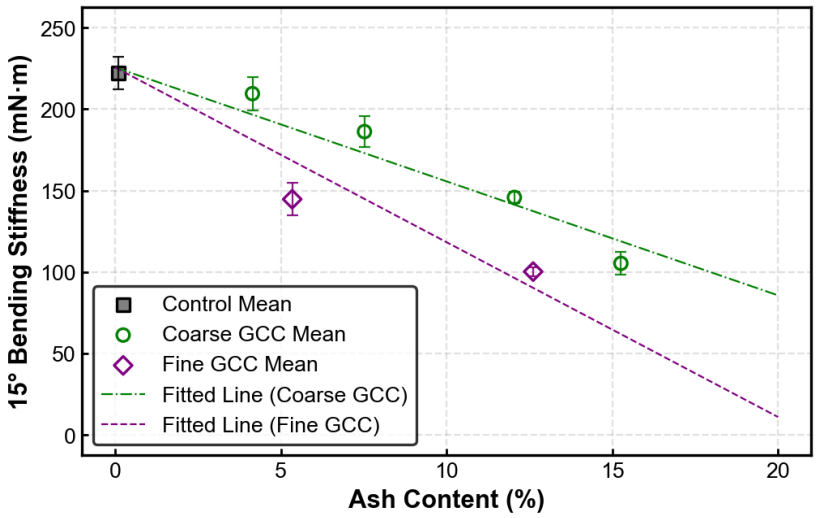

3-2.2. ANCOVA Slope estimates and 95% CI

Parameter	Estimate	95% CI (lower)	95% CI (upper)
γ_c	-6.995	-8.111	-5.879
γ_f	-10.729	-12.166	-9.292
γ_c - γ_f	3.734	2.489	4.980

3-2.3. ANCOVA hypothesis test table

H_0	F	df	p	Result
$\gamma_c = 0$	163.02	32	<0.001	Significant
$\gamma_f = 0$	231.25	32	<0.001	Significant
$\gamma_c = \gamma_f$	37.28	32	<0.001	Significant

3-2.4 ANCOVA fit summary

n	df_resid	R^2
35	32	0.890

3-2.5. ANCOVA assumption check

Test	Statistic	p	Result
Shapiro-Wilk	0.95	0.145	Not significant (normality not rejected)
Levene's test	3.30	0.050*	Significant (equal variances rejected)

*exact p = 0.04965

3-2.6. Representative residual plots (Q-Q plot, residuals vs fitted)

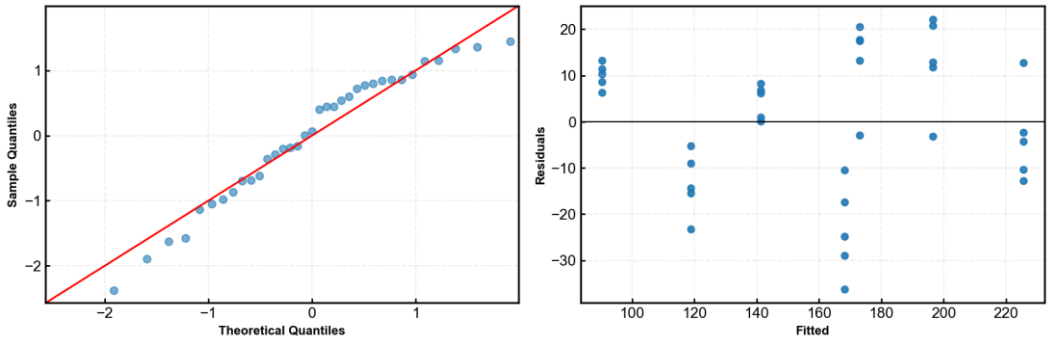

4. Burst Index

4-1. vs Filler Dosage

4-1.1. ANCOVA fitted line

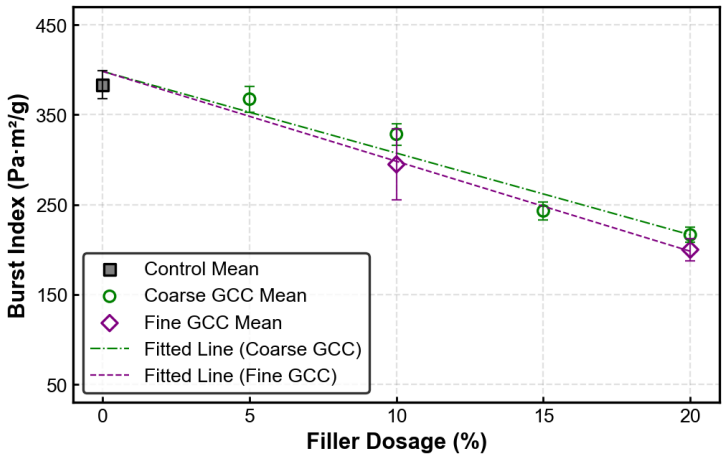

4-1.2. ANCOVA Slope estimates and 95% CI

Parameter	Estimate	95% CI (lower)	95% CI (upper)
γ_c	-9.088	-10.332	-7.844
γ_f	-10.000	-11.280	-8.721
$\gamma_c - \gamma_f$	0.913	-0.270	2.095

4-1.3. ANCOVA hypothesis test table

H_0	F	df	p	Result
$\gamma_c = 0$	221.46	32	<0.001	Significant
$\gamma_f = 0$	253.54	32	<0.001	Significant
$\gamma_c = \gamma_f$	2.47	32	0.126	Not significant

4-1.4. ANCOVA fit summary

n	df_resid	R^2
35	32	0.905

4-1.5. ANCOVA assumption check

Test	Statistic	p	Result
Shapiro-Wilk	0.99	0.998	Not significant (normality not rejected)
Levene's test	0.60	0.556	Not significant (equal variances not rejected)

4-1.6. Representative residual plots (Q-Q plot, residuals vs fitted)

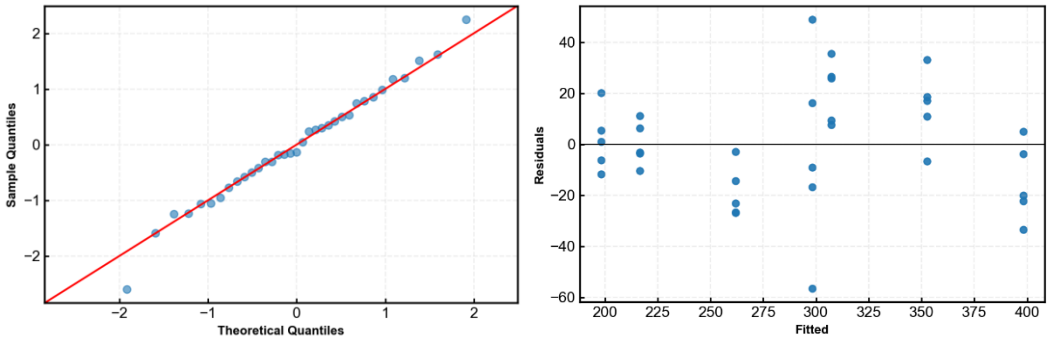

4-2. vs Ash Content

4-2.1. ANCOVA fitted line

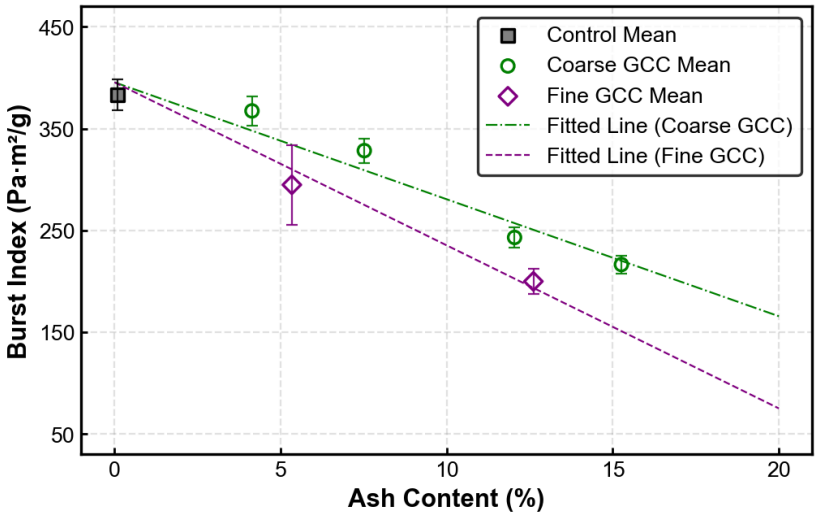

4-2.2. ANCOVA Slope estimates and 95% CI

Parameter	Estimate	95% CI (lower)	95% CI (upper)
γ_c	-11.490	-13.116	-9.864
γ_f	-16.016	-18.110	-13.922
$\gamma_c - \gamma_f$	4.526	2.711	6.341

4-2.3. ANCOVA hypothesis test table

H_0	F	df	p	Result
$\gamma_c = 0$	207.22	32	<0.001	Significant
$\gamma_f = 0$	242.75	32	<0.001	Significant
$\gamma_c = \gamma_f$	25.79	32	<0.001	Significant

4-2.4. ANCOVA fit summary

n	df_resid	R^2
35	32	0.901

4-2.5. ANCOVA assumption check

Test	Statistic	p	Result
Shapiro-Wilk	0.96	0.219	Not significant (normality not rejected)
Levene's test	0.93	0.404	Not significant (equal variances not rejected)

4-2.6. Representative residual plots (Q-Q plot, residuals vs. fitted)

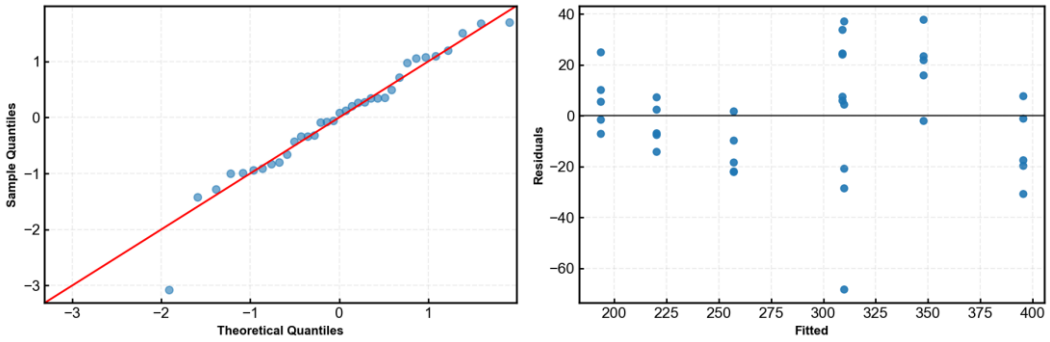

5. Tear Index

5-1. vs Filler Dosage

5-1.1. ANCOVA fitted line

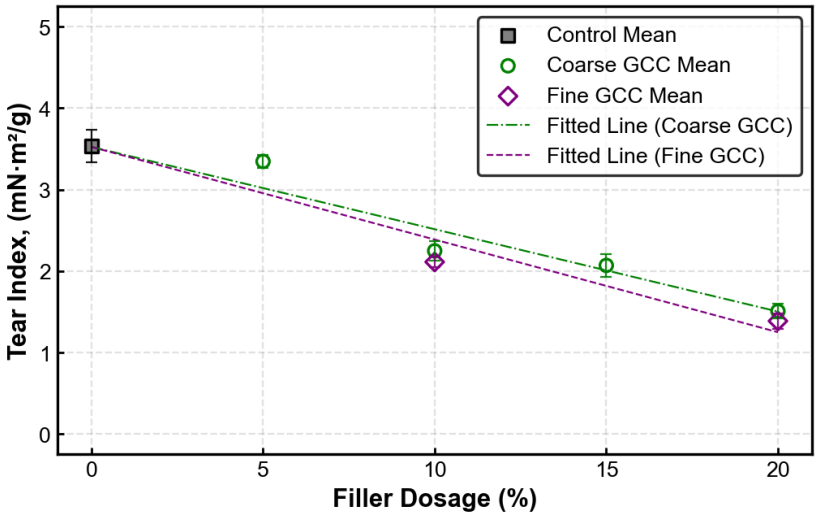

5-1.2. ANCOVA Slope estimates and 95% CI

Parameter	Estimate	95% CI (lower)	95% CI (upper)
γ_c	-0.101	-0.114	-0.088
γ_f	-0.114	-0.127	-0.100
γ_c - γ_f	0.013	0.000	0.025

5-1.3. ANCOVA hypothesis test table

H_0	F	df	p	Result
$\gamma_c = 0$	247.21	32	<0.001	Significant
$\gamma_f = 0$	296.02	32	<0.001	Significant
$\gamma_c = \gamma_f$	4.30	32	0.046	Significant

5-1.4. ANCOVA fit summary

n	df_resid	R^2
35	32	0.916

5-1.5. ANCOVA assumption check

Test	Statistic	p	Result
Shapiro-Wilk	0.97	0.554	Not significant (normality not rejected)
Levene's test	0.60	0.557	Not significant (equal variances not rejected)

5-1.6. Representative residual plots (Q-Q plot, residuals vs fitted)

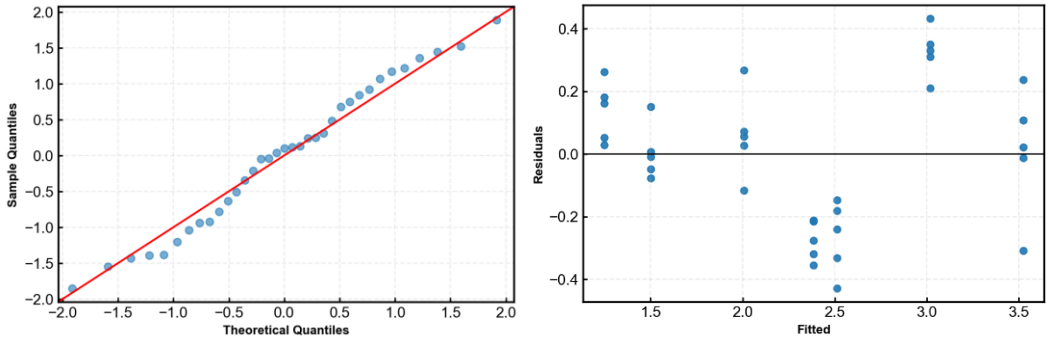

5-2. vs. Ash Content

5-2.1. ANCOVA fitted line

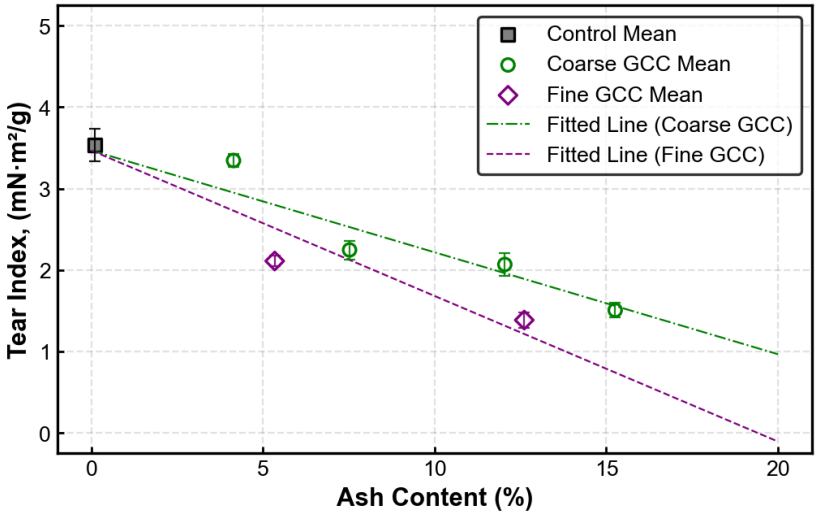

5-2.2. ANCOVA Slope estimates and 95% CI

Parameter	Estimate	95% CI (lower)	95% CI (upper)
γ_c	-0.125	-0.145	-0.105
γ_f	-0.179	-0.205	-0.152
$\gamma_c - \gamma_f$	0.054	0.031	0.076

5-2.3. ANCOVA hypothesis test table

H_0	F	df	p	Result
$\gamma_c = 0$	156.63	32	<0.001	Significant
$\gamma_f = 0$	192.72	32	<0.001	Significant
$\gamma_c = \gamma_f$	23.08	32	<0.001	Significant

5-2.4. ANCOVA fit summary

n	df_resid	R^2
35	32	0.877

5-2.5. ANCOVA assumption check

Test	Statistic	p	Result
Shapiro-Wilk	0.96	0.281	Not significant (normality not rejected)
Levene's test	2.41	0.106	Not significant (equal variances not rejected)

5-2.6. Representative residual plots (Q-Q plot, residuals vs. fitted)

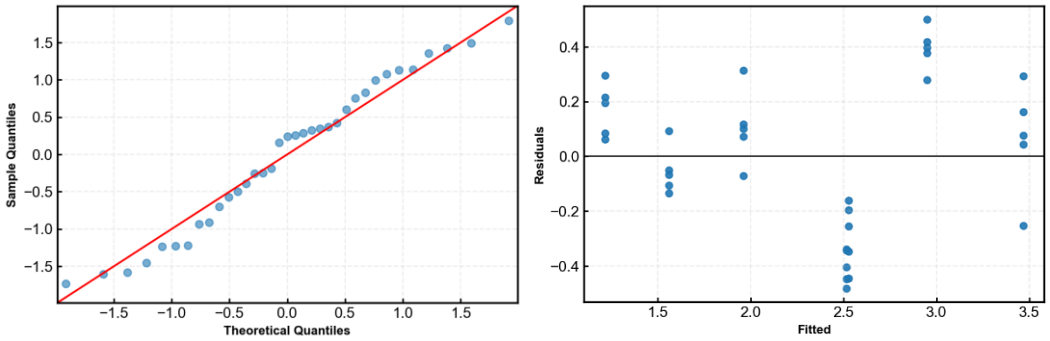

6. Tensile Index

6-1. vs Filler Dosage

6-1.1. ANCOVA fitted line

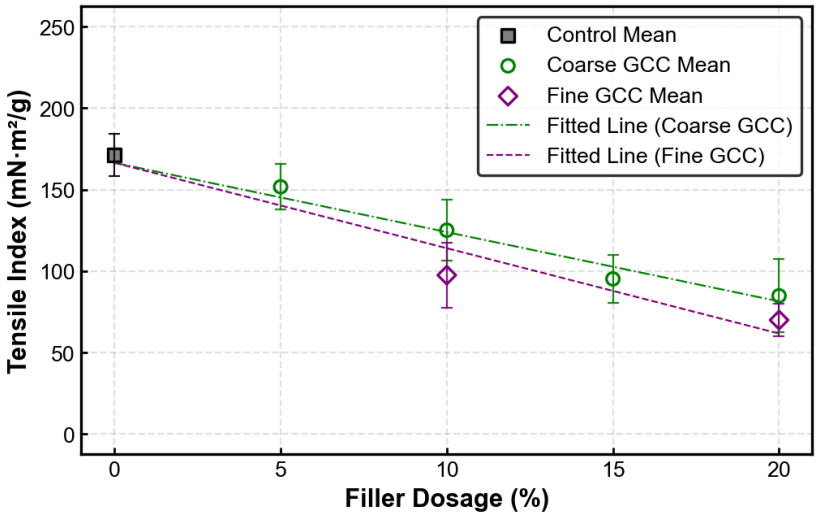

6-1.2. ANCOVA Slope estimates and 95% CI

Parameter	Estimate	95% CI (lower)	95% CI (upper)
γ_c	-4.251	-5.237	-3.265
γ_f	-5.239	-6.254	-4.225
$\gamma_c - \gamma_f$	0.988	0.050	1.926

6-1.3. ANCOVA hypothesis test table

H_0	F	df	p	Result
$\gamma_c = 0$	77.07	32	<0.001	Significant
$\gamma_f = 0$	110.68	32	<0.001	Significant
$\gamma_c = \gamma_f$	4.61	32	0.040	Significant

6-1.4. ANCOVA fit summary

n	df_resid	R^2
35	32	0.793

6-1.5. ANCOVA assumption check

Test	Statistic	p	Result
Shapiro-Wilk	0.99	0.973	Not significant (normality not rejected)
Levene's test	0.38	0.690	Not significant (equal variances not rejected)

6-1.6. Representative residual plots (Q-Q plot, residuals vs. fitted)

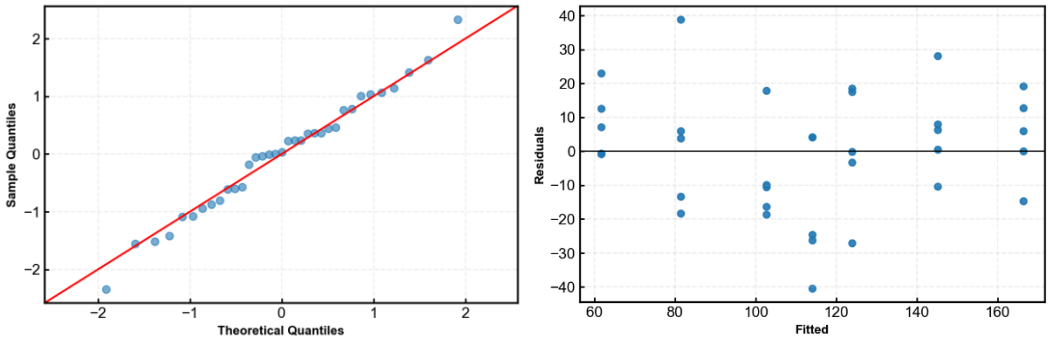

6-2. vs. Ash Content

6-2.1. ANCOVA fitted line

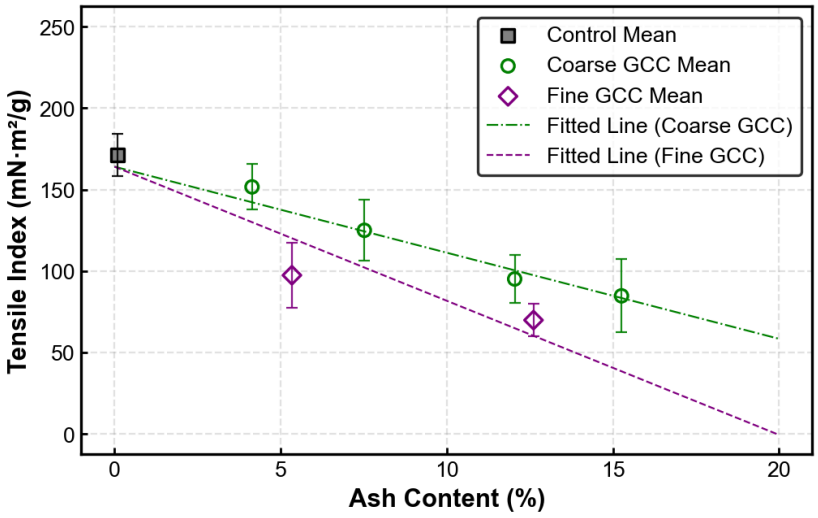

6-2.2. ANCOVA Slope estimates and 95% CI

Parameter	Estimate	95% CI (lower)	95% CI (upper)
γ_c	-5.283	-6.637	-3.930
γ_f	-8.233	-9.976	-6.489
γ_c - γ_f	2.949	1.438	4.460

6-2.3. ANCOVA hypothesis test table

H_0	F	df	p	Result
$\gamma_c = 0$	63.22	32	<0.001	Significant
$\gamma_f = 0$	92.54	32	<0.001	Significant
$\gamma_c = \gamma_f$	15.80	32	<0.001	Significant

6-2.4. ANCOVA fit summary

n	df_resid	R^2
35	32	0.763

6-2.5. ANCOVA assumption check

Test	Statistic	p	Result
Shapiro-Wilk	0.99	0.947	Not significant (normality not rejected)
Levene's test	0.56	0.578	Not significant (equal variances not rejected)

6-2.6. Representative residual plots (Q-Q plot, residuals vs. fitted)

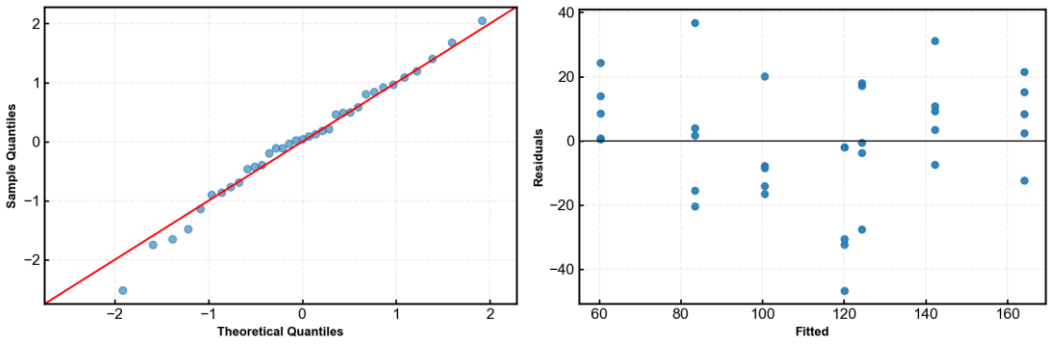

7. Canadian Standard Freeness

7-1. vs Filler Dosage

7-1.1. ANCOVA fitted line

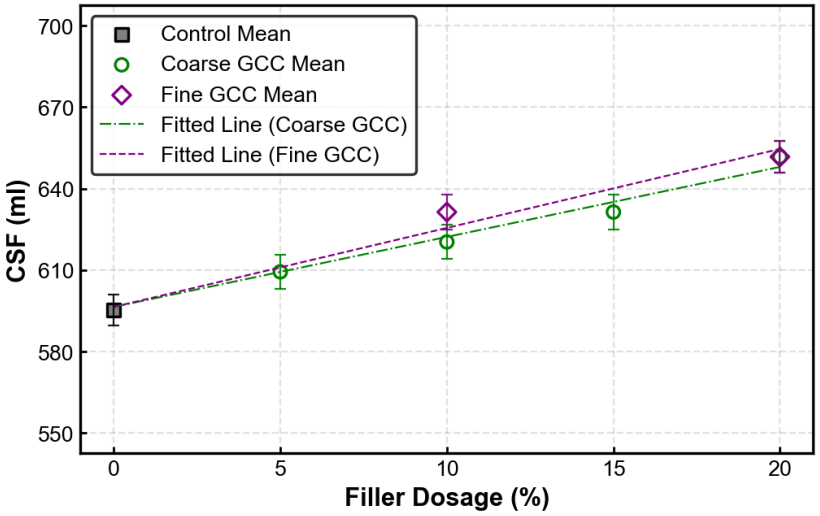

7-1.2. ANCOVA Slope estimates and 95% CI

Parameter	Estimate	95% CI (lower)	95% CI (upper)
γ_c	2.577	2.100	3.053
γ_f	2.908	2.418	3.398
$\gamma_c - \gamma_f$	-0.332	-0.785	0.121

7-1.3. ANCOVA hypothesis test table

H_0	F	df	p	Result
$\gamma_c = 0$	129.16	18	<0.001	Significant
$\gamma_f = 0$	155.58	18	<0.001	Significant
$\gamma_c = \gamma_f$	2.37	18	0.141	Not significant

7-1.4. ANCOVA fit summary

n	df_resid	R^2
21	18	0.911

7-1.5. ANCOVA assumption check

Test	Statistic	p	Result
Shapiro-Wilk	0.96	0.557	Not significant (normality not rejected)
Levene's test	0.15	0.860	Not significant (equal variances not rejected)

7-1.6. Representative residual plots (Q-Q plot, residuals vs. fitted)

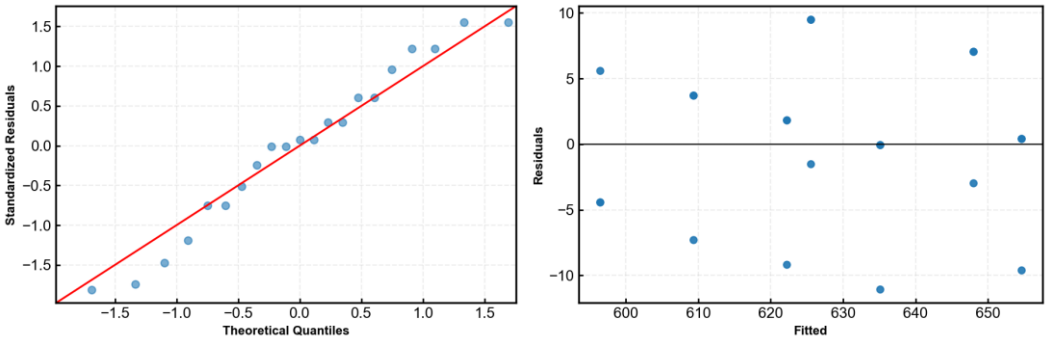

7-2. vs. Ash Content

7-2.1. ANCOVA fitted line

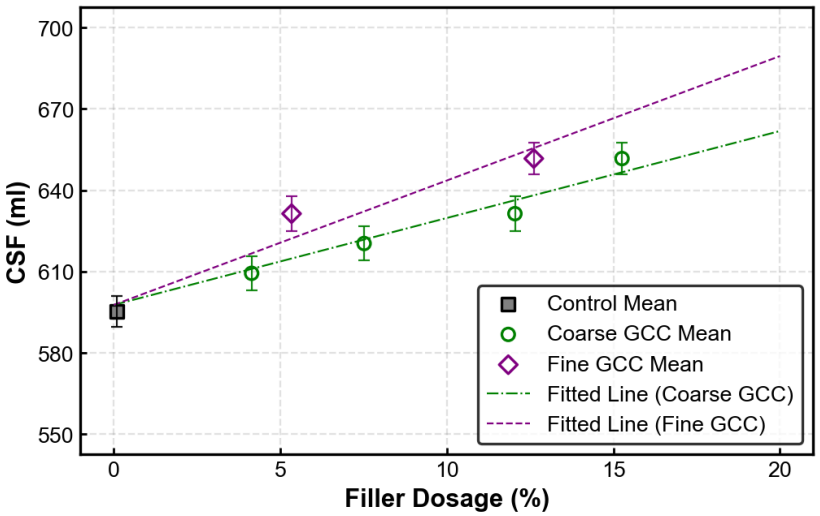

7-2.2. ANCOVA Slope estimates and 95% CI

Parameter	Estimate	95% CI (lower)	95% CI (upper)
γ_c	3.207	2.501	3.913
γ_f	4.590	3.681	5.499
$\gamma_c - \gamma_f$	-1.382	-2.171	-0.594

7-2.3. ANCOVA hypothesis test table

H_0	F	df	p	Result
$\gamma_c = 0$	91.12	18	<0.001	Significant
$\gamma_f = 0$	112.51	18	<0.001	Significant
$\gamma_c = \gamma_f$	13.58	18	0.002	Significant

7-2.4. ANCOVA fit summary

n	df_resid	R^2
21	18	0.880

7-2.5. ANCOVA assumption check

Test	Statistic	p	Result
Shapiro-Wilk	0.96	0.495	Not significant (normality not rejected)
Levene's test	0.46	0.640	Not significant (equal variances not rejected)

7-2.6. Representative residual plots (Q-Q plot, residuals vs. fitted)

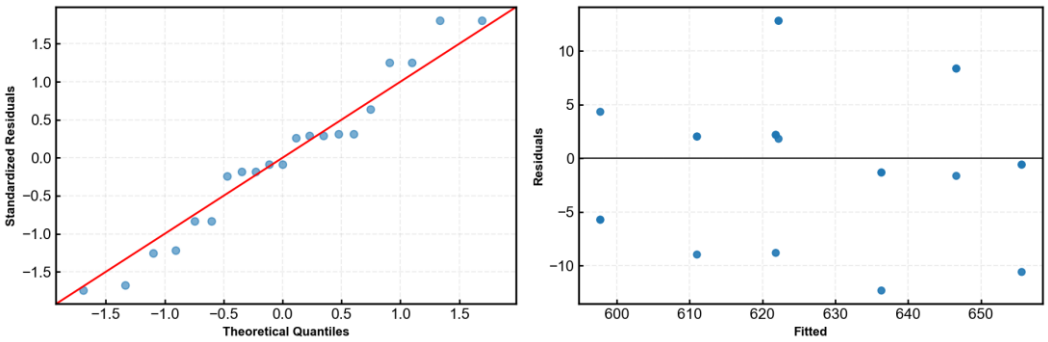

8. $DE_{forming}$

8-1. vs. Filler Dosage

8-1.1. ANCOVA fitted line

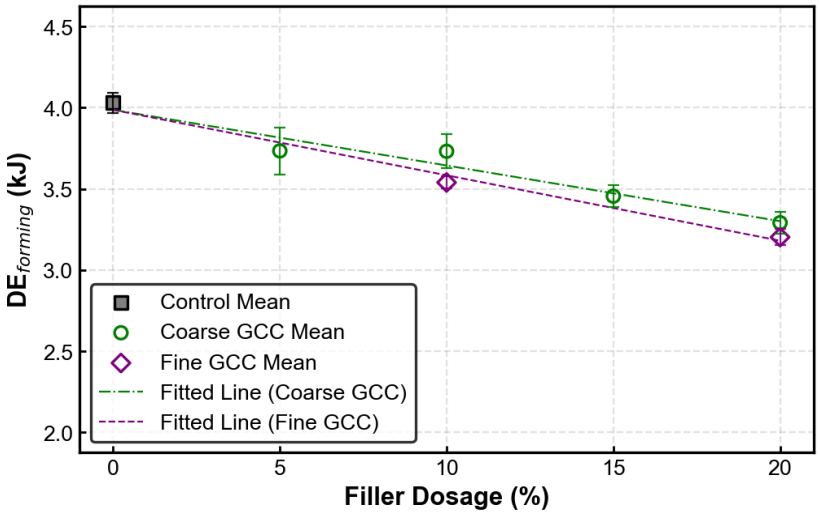

8-1.2. ANCOVA Slope estimates and 95% CI

Parameter	Estimate	95% CI (lower)	95% CI (upper)
γ_c	-0.034	-0.041	-0.027
γ_f	-0.040	-0.047	-0.033
$\gamma_c - \gamma_f$	0.006	0.000	0.013

8-1.3. ANCOVA hypothesis test table

H_0	F	df	p	Result
$\gamma_c = 0$	110.52	18	<0.001	Significant
$\gamma_f = 0$	144.53	18	<0.001	Significant
$\gamma_c = \gamma_f$	3.79	18	0.067	Not significant

8-1.4. ANCOVA fit summary

n	df_resid	R^2
21	18	0.902

8-1.5. ANCOVA assumption check

Test	Statistic	p	Result
Shapiro-Wilk	0.98	0.877	Not significant (normality not rejected)
Levene's test	1.62	0.225	Not significant (equal variances not rejected)

8-1.6. Representative residual plots (Q-Q plot, residuals vs. fitted)

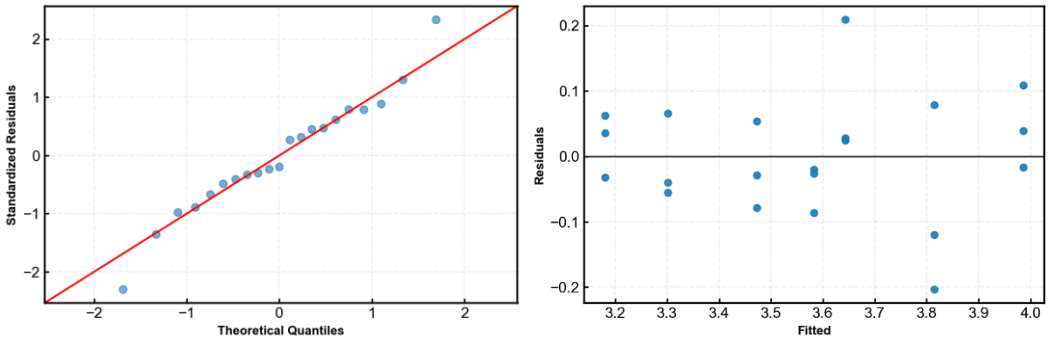

8-2. vs. Ash Content

8-2.1. ANCOVA fitted line

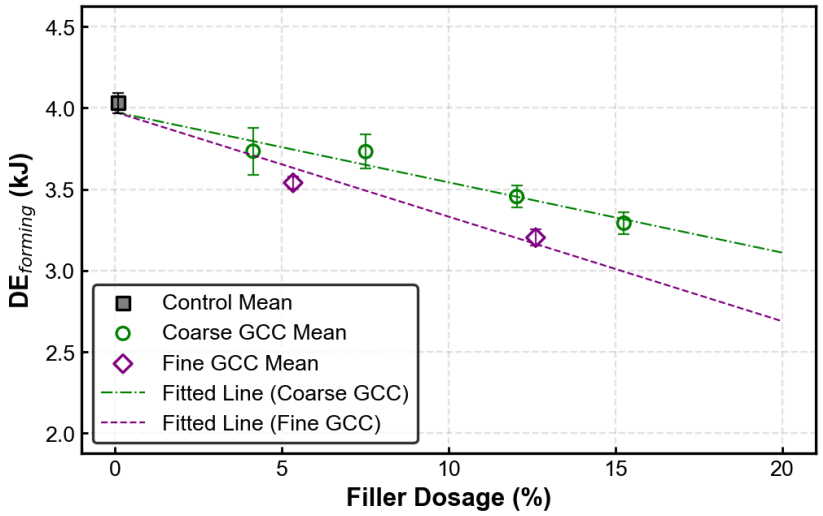

8-2.2. ANCOVA Slope estimates and 95% CI

Parameter	Estimate	95% CI (lower)	95% CI (upper)
γ_c	-0.043	-0.052	-0.034
γ_f	-0.064	-0.076	-0.052
$\gamma_c - \gamma_f$	0.021	0.011	0.031

8-2.3. ANCOVA hypothesis test table

H_0	F	df	p	Result
$\gamma_c = 0$	97.39	18	<0.001	Significant
$\gamma_f = 0$	130.04	18	<0.001	Significant
$\gamma_c = \gamma_f$	18.61	18	<0.001	Significant

8-2.4. ANCOVA fit summary

n	df_resid	R^2
21	18	0.892

8-2.5. ANCOVA assumption check

Test	Statistic	p	Result
Shapiro-Wilk	0.99	0.995	Not significant (normality not rejected)
Levene's test	0.58	0.568	Not significant (equal variances not rejected)

8-2.6. Representative residual plots (Q-Q plot, residuals vs. fitted)

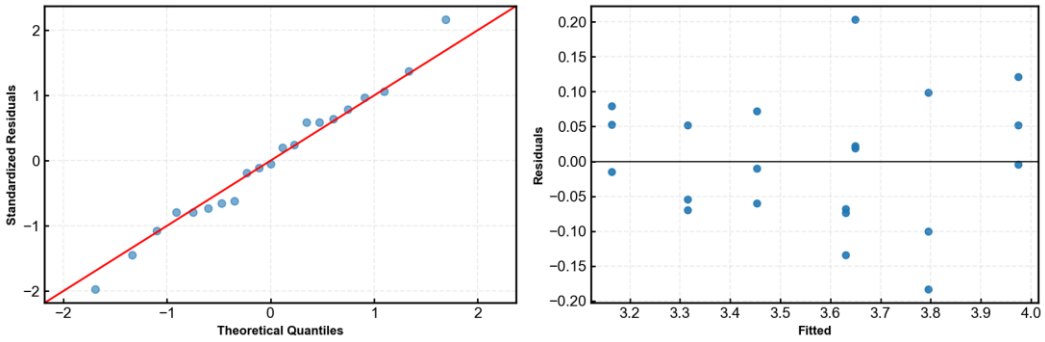

9. $DE_{HP-1min}$

9-1. vs Filler Dosage

9-1.1. ANCOVA fitted line

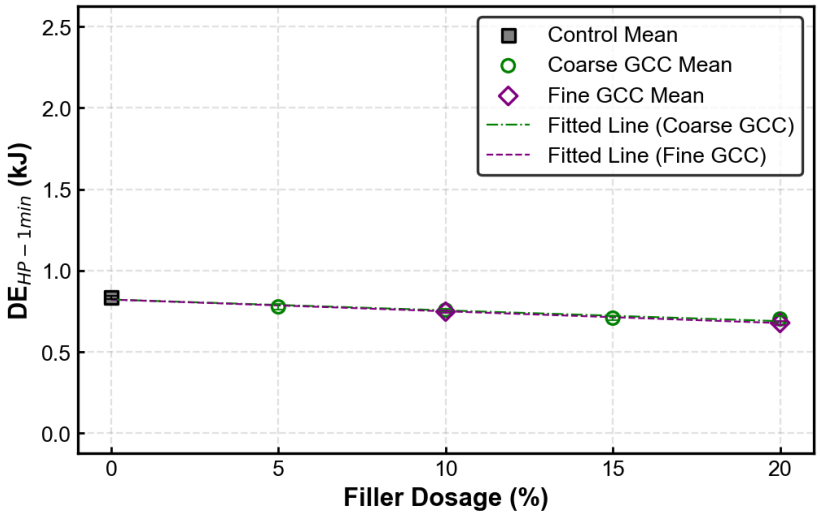

9-1.2. ANCOVA Slope estimates and 95% CI

Parameter	Estimate	95% CI (lower)	95% CI (upper)
γ_c	-0.007	-0.008	-0.006
γ_f	-0.007	-0.008	-0.006
γ_c - γ_f	0.001	0.000	0.002

9-1.3. ANCOVA hypothesis test table

H_0	F	df	P	Result
$\gamma_c = 0$	161.63	18	<0.001	Significant
$\gamma_f = 0$	181.07	18	<0.001	Significant
$\gamma_c = \gamma_f$	1.40	18	0.252	Not significant

9-1.4. ANCOVA fit summary

n	df_resid	R^2
21	18	0.924

9-1.5. ANCOVA assumption check

Test	Statistic	p	Result
Shapiro-Wilk	0.95	0.338	Not significant (normality not rejected)
Levene's test	1.87	0.183	Not significant (equal variances not rejected)

9-1.6. Representative residual plots (Q-Q plot, residuals vs. fitted)

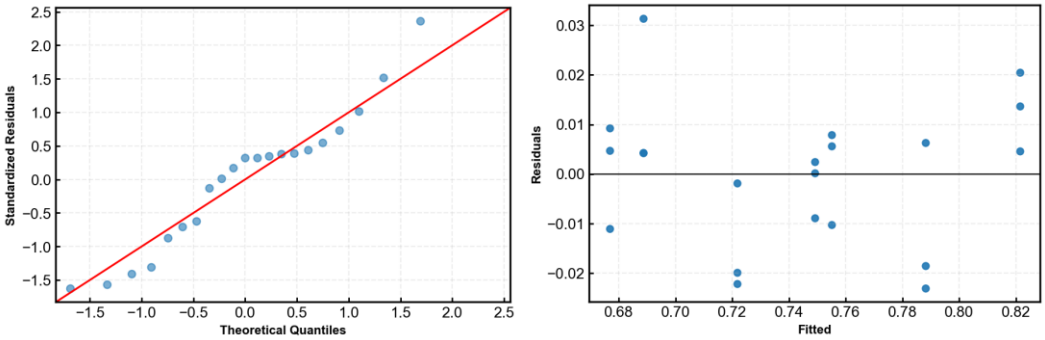

9-2. vs. Ash Content

9-2.1. ANCOVA fitted line

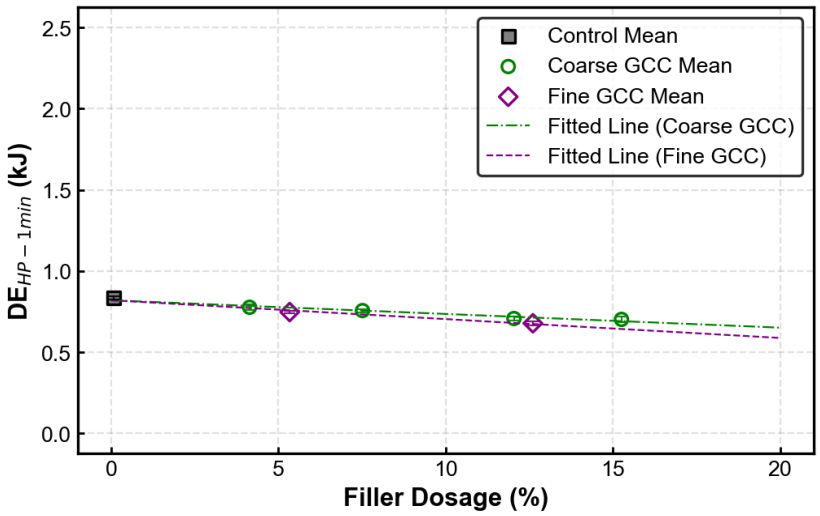

9-2.2. ANCOVA Slope estimates and 95% CI

Parameter	Estimate	95% CI (lower)	95% CI (upper)
γ_c	-0.008	-0.010	-0.007
γ_f	-0.012	-0.013	-0.010
γ_c - γ_f	0.003	0.002	0.005

9-2.3. ANCOVA hypothesis test table

H_0	F	df	p	Result
$\gamma_c = 0$	164.88	18	<0.001	Significant
$\gamma_f = 0$	188.14	18	<0.001	Significant
$\gamma_c = \gamma_f$	18.67	18	<0.001	Significant

9-2.4. ANCOVA fit summary

n	df_resid	R^2
21	18	0.927

9-2.5. ANCOVA assumption check

Test	Statistic	p	Result
Shapiro-Wilk	0.96	0.433	Not significant (normality not rejected)
Levene's test	0.60	0.561	Not significant (equal variances not rejected)

9-2.6. Representative residual plots (Q-Q plot, residuals vs fitted)

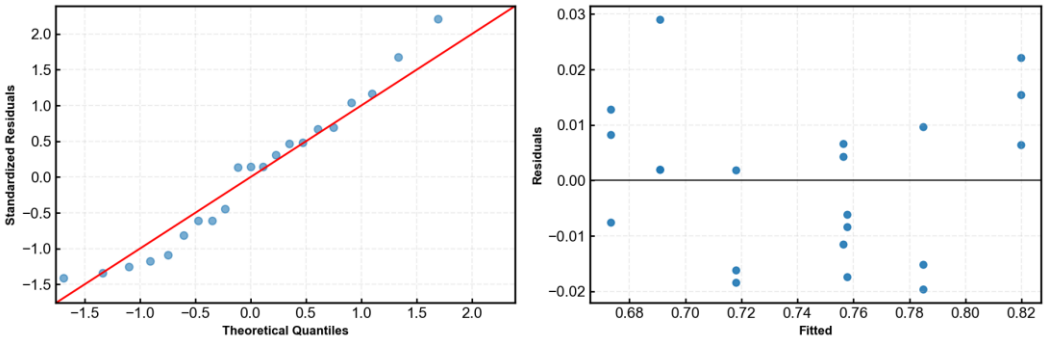

10. $SEC_{forming}$

$SEC_{forming}$ showed minimal dependence on filler dosage (Fig. 6), resulting in a low R^2 in the linear ANCOVA model. This does not indicate model misspecification; rather, it reflects that the between-condition (dose-related) variance is small relative to specimen-to-specimen variability. Shapiro–Wilk showed a mild departure from normality. However, residual diagnostics did not show systematic curvature or pronounced heteroscedasticity; thus, conclusions were interpreted with the mild non-normality noted.

10-1. vs Filler Dosage

10-1.1. ANCOVA fitted line

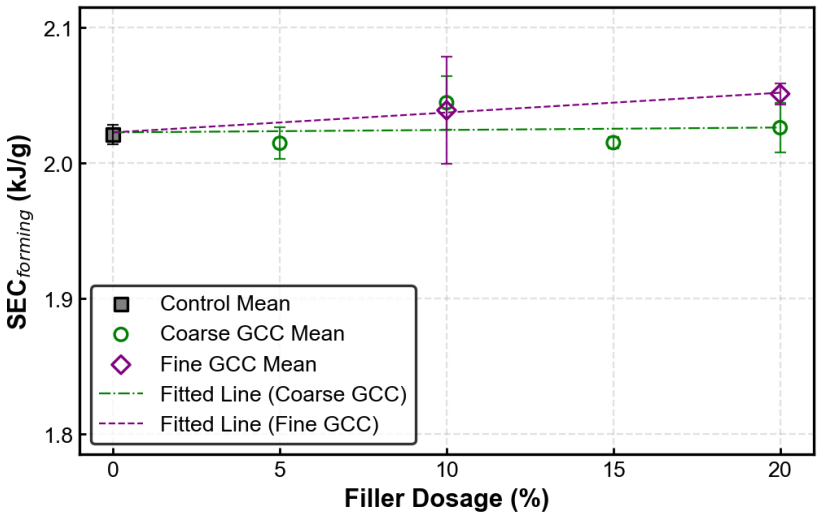

10-1.2. ANCOVA Slope estimates and 95% CI

Parameter	Estimate	95% CI (lower)	95% CI (upper)
γ_c	<0.001	-0.001	0.002
γ_f	0.001	<0.001	0.003
$\gamma_c - \gamma_f$	-0.001	-0.003	<0.001

10-1.3. ANCOVA hypothesis test table

H_0	F	df	p	Result
$\gamma_c = 0$	0.07	18	0.797	Not significant
$\gamma_f = 0$	4.27	18	0.053	Not significant
$\gamma_c = \gamma_f$	3.85	18	0.065	Not significant

10-1.4. ANCOVA fit summary

n	df_resid	R^2
21	18	0.233

10-1.5. ANCOVA assumption check

Test	Statistic	p	Result
Shapiro-Wilk	0.91	0.049	Significant (normality rejected)
Levene's test	0.84	0.449	Not significant (equal variances not rejected)

10-1.6. Representative residual plots (Q-Q plot, residuals vs. fitted)

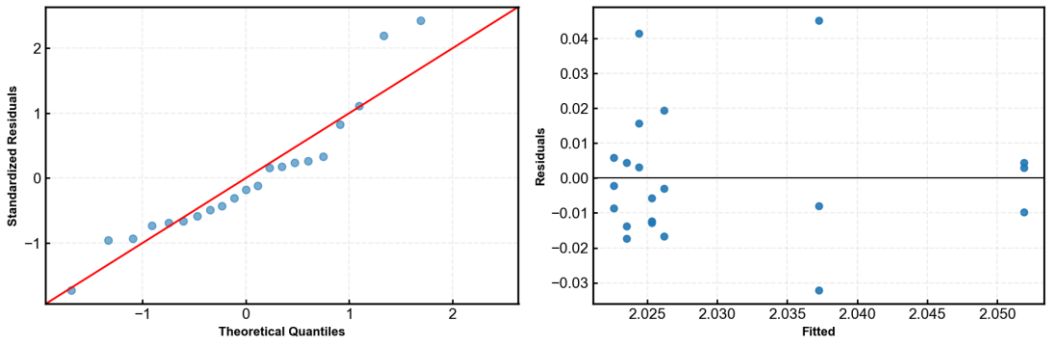

10-2. vs. Ash Content

10-2.1. ANCOVA fitted line

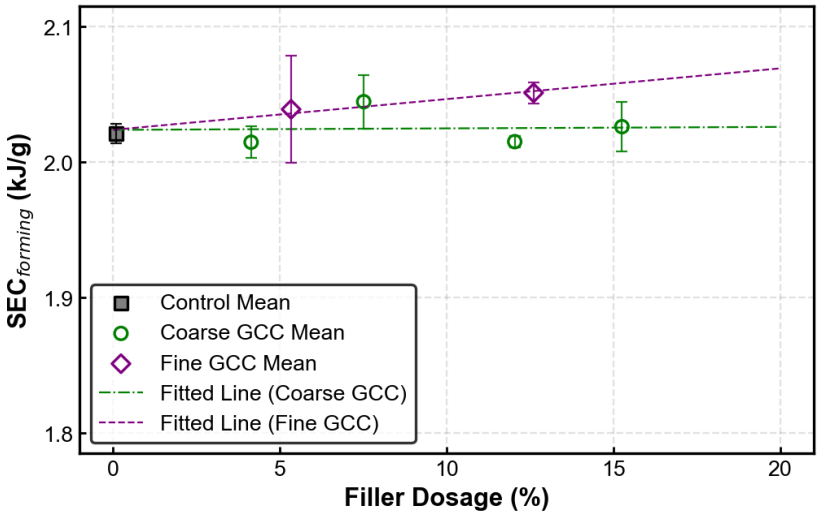

10-2.2. ANCOVA Slope estimates and 95% CI

Parameter	Estimate	95% CI (lower)	95% CI (upper)
γ_c	<0.001	-0.002	0.002
γ_f	0.002	<0.001	0.005
$\gamma_c - \gamma_f$	-0.002	-0.004	<0.001

10-2.3. ANCOVA hypothesis test table

H_0	F	df	p	Result
$\gamma_c = 0$	0.02	18	0.904	Not significant
$\gamma_f = 0$	3.96	18	0.062	Not significant
$\gamma_c = \gamma_f$	4.78	18	0.042	Significant

10-2.4. ANCOVA fit summary

n	df_resid	R^2
21	18	0.228

10-2.5. ANCOVA assumption check

Test	Statistic	p	Result
Shapiro-Wilk	0.90	0.034	Significant (normality rejected)
Levene's test	0.79	0.468	Not significant (equal variances not rejected)

10-2.6. Representative residual plots (Q-Q plot, residuals vs. fitted)

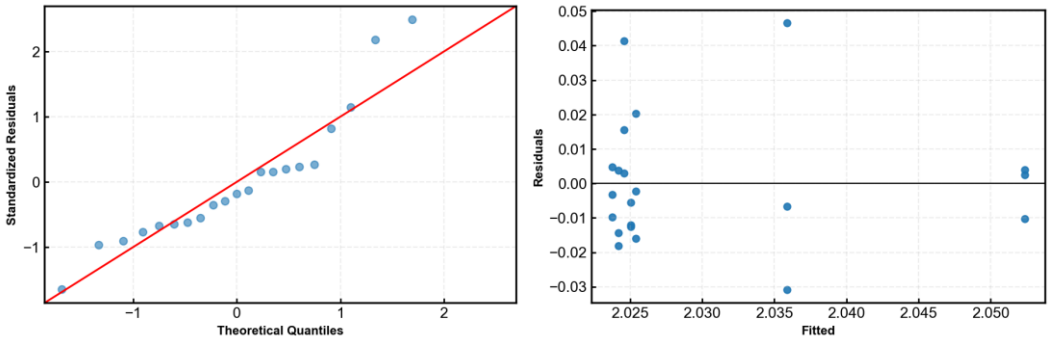

11. $SEC_{HP-1min}$

The ANCOVA model yielded a low R^2, consistent with the visually weak dose-response. Normality and homoscedasticity diagnostics were satisfactory, supporting the validity of the parametric inference. The low R^2 primarily reflects limited dose-related explanatory signal rather than diagnostic failure.

11-1. vs Filler Dosage

11-1.1. ANCOVA fitted line

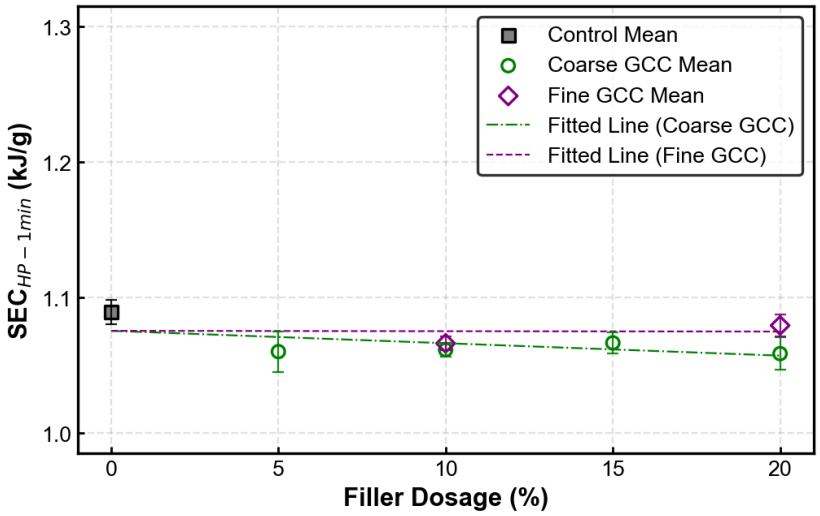

11-1.2. ANCOVA Slope estimates and 95% CI

Parameter	Estimate	95% CI (lower)	95% CI (upper)
γ_c	-0.001	-0.002	<0.001
γ_f	<0.001	-0.001	0.001
γ_c - γ_f	-0.001	-0.002	<0.001

11-1.3. ANCOVA hypothesis test table

H_0	F	df	p	Result
$\gamma_c = 0$	4.61	18	0.046	Significant
$\gamma_f = 0$	0.00	18	0.951	Not significant
$\gamma_c = \gamma_f$	4.80	18	0.042	Significant

11-1.4. ANCOVA fit summary

n	df_resid	R^2
21	18	0.266

11-1.5. ANCOVA assumption check

Test	Statistic	p	Result
Shapiro-Wilk	0.98	0.958	Not significant (normality not rejected)
Levene's test	0.30	0.748	Not significant (equal variances not rejected)

11-1.6. Representative residual plots (Q-Q plot, residuals vs fitted)

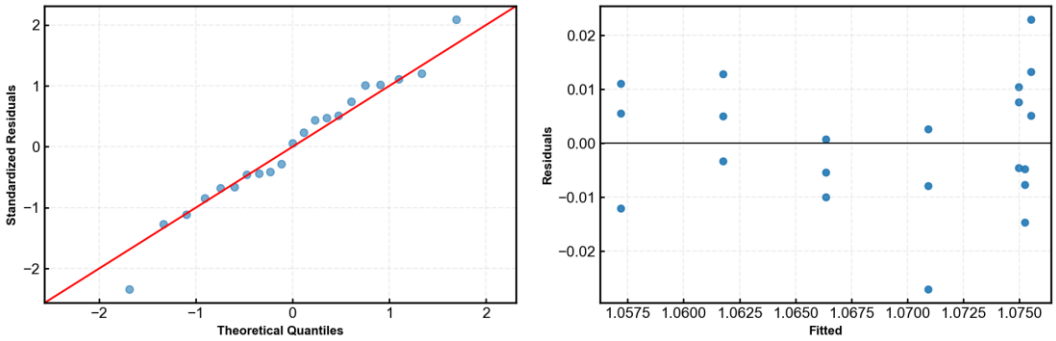

11-2. vs Ash Content

11-2.1. ANCOVA fitted line

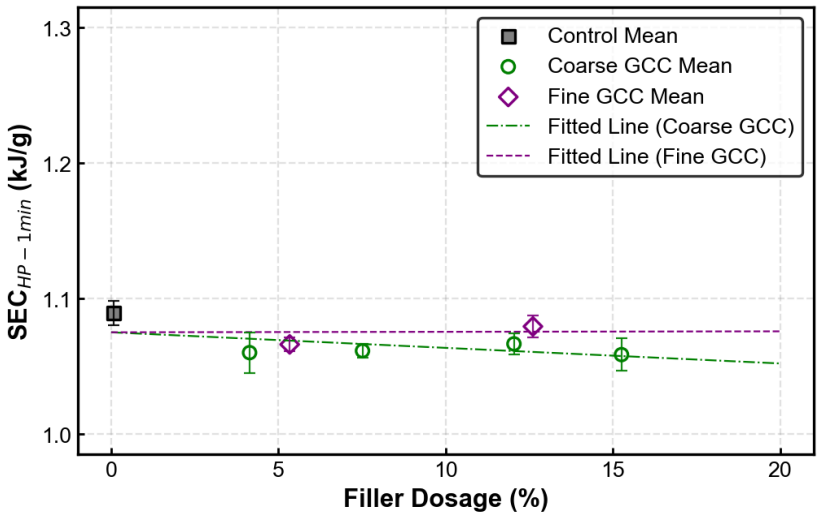

11-2.2. ANCOVA Slope estimates and 95% CI

Parameter	Estimate	95% CI (lower)	95% CI (upper)
γ_c	-0.001	-0.002	<0.001
γ_f	<0.001	-0.001	0.002
γ_c - γ_f	-0.001	-0.002	<0.001

11-2.3. ANCOVA hypothesis test table

H_0	F	df	p	Result
$\gamma_c = 0$	4.42	18	0.050	Significant
$\gamma_f = 0$	0.00	18	0.960	Not significant
$\gamma_c = \gamma_f$	3.77	18	0.068	Not significant

11-2.4. ANCOVA fit summary

n	df_resid	R^2
21	18	0.265

11-2.5. ANCOVA assumption check

Test	Statistic	p	Result
Shapiro-Wilk	0.98	0.977	Not significant (normality not rejected)
Levene's test	0.32	0.733	Not significant (equal variances not rejected)

11-2.6. Representative residual plots (Q-Q plot, residuals vs. fitted)

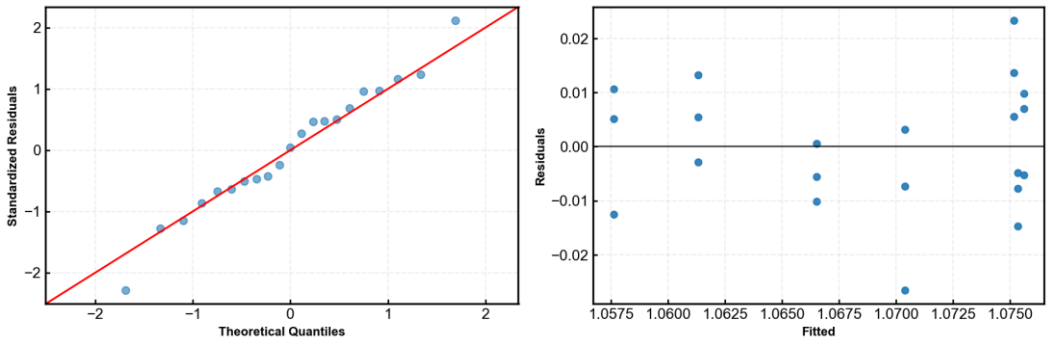

B. One-way ANOVA and Dunnett's Post-hoc Test
1. Porosity

1.1. One-way ANOVA results

	Sum_sq	df	F	PR(>F)
Between (Treatment; 7 levels, incl. Control)	52.74	6	27.41	<0.001
Residual	6.74	21	-	-

1.2. Effect-size reports

η²	ω²
0.887	0.850

1.3. ANOVA assumption check

Test	Statistic	p	Result
Shapiro-Wilk	0.94	0.096	Not significant (normality not rejected)
Levene's test	1.14	0.372	Not significant (homogeneity not rejected)

1.4. ANOVA fit summary

n	df_resid	R^2 (OLS)
28	21	0.887

1.5. Representative residual plots (OLS Residuals): Q-Q plot, residuals vs fitted

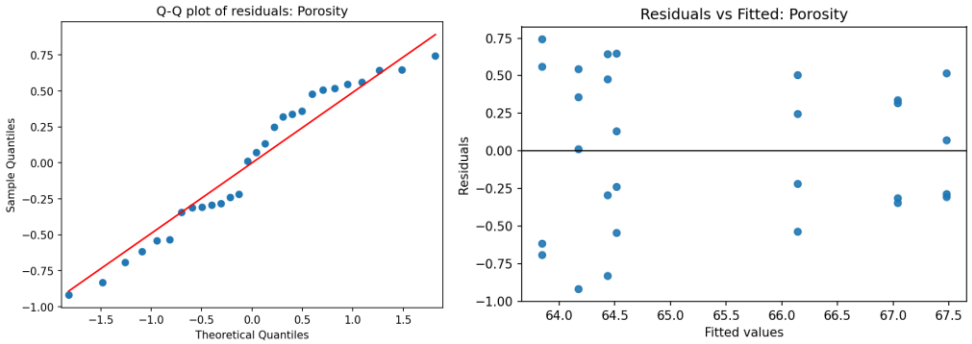

1.6. Dunnett's post-hoc test

Comparison (vs control)	ΔMean	95% CI (lower)	95% CI (upper)	Statistic	p	Result
Coarse GCC 5%	-0.33	-1.45	0.79	-0.82	0.910	Rejected
Coarse GCC 10%	0.26	-0.85	1.38	0.66	0.965	Rejected
Coarse GCC 15%	1.97	0.85	3.09	4.92	<0.001	Accepted
Coarse GCC 20%	2.86	1.75	3.98	7.15	<0.001	Accepted
Fine GCC 10%	0.34	-0.77	1.46	0.86	0.895	Rejected
Fine GCC 20%	3.31	2.19	4.42	8.25	<0.001	Accepted

2. Gurley

2.1. One-way ANOVA results

	Sum_sq	df	F	PR(>F)
Between (Treatment; 7 levels, incl. Control)	31.96	6	49.56	<0.001
Residual	2.26	21	-	-

2.2. Effect-size reports

η²	ω²
0.934	0.912

2.3. ANOVA assumption check

Test	Statistic	p	Result
Shapiro-Wilk	0.95	0.232	Not significant (normality not rejected)
Levene's test	2.39	0.064	Not significant (homogeneity not rejected)

2.4. ANOVA fit summary

n	df_resid	R^2 (OLS)
28	21	0.934

2.5. Representative residual plots (OLS Residuals): Q-Q plot, residuals vs. fitted

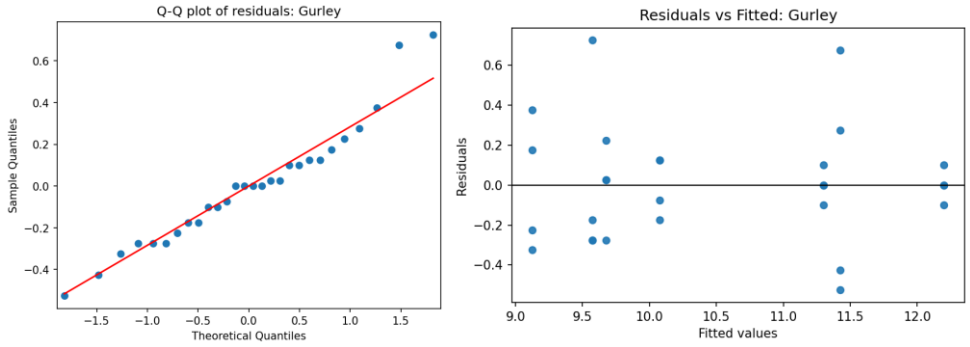

2.6. Dunnett's post-hoc test

Comparison (vs control)	ΔMean	95% CI (lower)	95% CI (upper)	Statistic	p	Result
Coarse GCC 5%	1.73	1.08	2.37	7.44	<0.001	Accepted
Coarse GCC 10%	2.63	1.98	3.27	11.32	<0.001	Accepted
Coarse GCC 15%	0.10	-0.55	0.75	0.43	0.996	Rejected
Coarse GCC 20%	0.50	-0.15	1.15	2.16	0.173	Rejected
Fine GCC 10%	1.85	1.20	2.50	7.98	<0.001	Accepted
Fine GCC 20%	-0.45	-1.10	0.20	-1.94	0.251	Rejected

3. CSF

3.1. One-way ANOVA results

	Sum_sq	df	F	PR(>F)
Between (Treatment; 7 levels, incl. Control)	7839.62	6	35.00	<0.001
Residual	522.67	14	-	-

3.2. Effect-size reports

η^2	ω^2
0.937	0.907

3.3. ANOVA assumption check

Test	Statistic	p	Result
Shapiro-Wilk	0.74	<0.001	Significant (normality rejected)
Levene's test	0.00*	1.000*	Not significant (homogeneity not rejected)

*exact statistic = 0.0026, p > 0.999

3.4. ANOVA fit summary

n	df_resid	R^2 (OLS)
21	14	0.938

3.5. Representative residual plots (OLS Residuals): Q-Q plot, residuals vs fitted

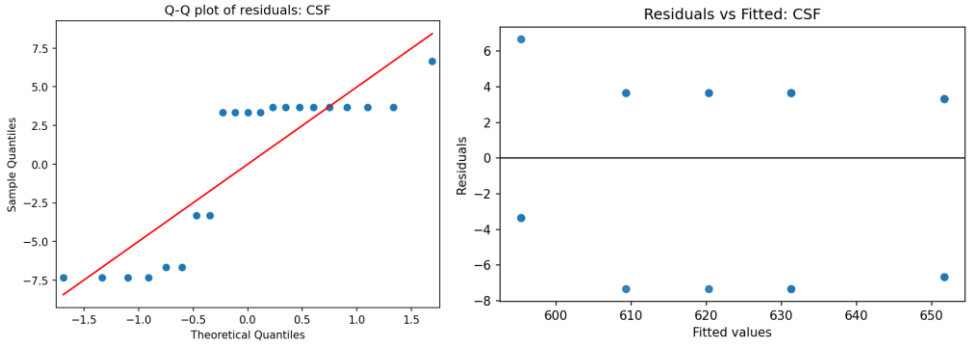

3.6. Dunnett's post-hoc test

Comparison (vs control)	ΔMean	95% CI (lower)	95% CI (upper)	Statistic	p	Result
Coarse GCC 5%	14.00	-0.53	28.53	2.81	0.061	Rejected
Coarse GCC 10%	25.00	10.47	39.53	5.01	0.001	Accepted
Coarse GCC 15%	36.00	21.47	50.53	7.22	<0.001	Accepted
Coarse GCC 20%	56.33	41.80	70.87	11.29	<0.001	Accepted
Fine GCC 10%	36.00	21.47	50.53	7.22	<0.001	Accepted
Fine GCC 20%	56.33	41.80	70.87	11.29	<0.001	Accepted

4. $DE_{forming}$

4.1. One-way ANOVA results

	Sum_sq	df	F	PR(>F)
Between (Treatment; 7 levels, incl. Control)	1.48	6	35.39	<0.001
Residual	0.10	14	-	-

4.2. Effect-size reports

η^2	ω^2
0.938	0.908

4.3. ANOVA assumption check

Test	Statistic	p	Result
Shapiro-Wilk	0.95	0.305	Not significant (normality not rejected)
Levene's test	0.40	0.866	Not significant (homogeneity not rejected)

4.4. ANOVA fit summary

n	df_resid	R^2 (OLS)
21	14	0.938

4.5. Representative residual plots (OLS Residuals): Q-Q plot, residuals vs fitted

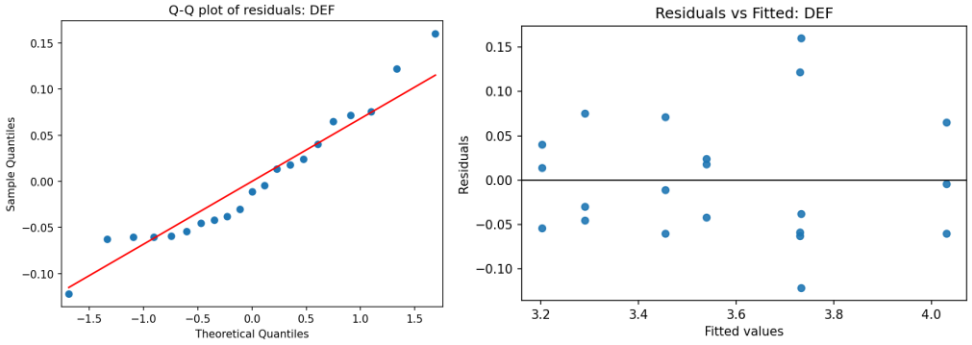

4.6. Dunnett's post-hoc test

Comparison (vs control)	ΔMean	95% CI (lower)	95% CI (upper)	Statistic	p	Result
Coarse GCC 5%	-0.30	-0.50	-0.10	-4.36	0.003	Accepted
Coarse GCC 10%	-0.30	-0.50	-0.10	-4.40	0.003	Accepted
Coarse GCC 15%	-0.58	-0.77	-0.38	-8.46	<0.001	Accepted
Coarse GCC 20%	-0.74	-0.94	-0.54	-10.86	<0.001	Accepted
Fine GCC 10%	-0.49	-0.69	-0.29	-7.22	<0.001	Accepted
Fine GCC 20%	-0.83	-1.03	-0.63	-12.16	<0.001	Accepted

5. $DE_{HP\text{-}1min}$

5.1. One-way ANOVA results

	Sum_sq	df	F	PR(>F)
Between (Treatment; 7 levels, incl. Control)	0.05	6	63.65	<0.001
Residual	0.00	14	-	-

5.2. Effect-size reports

η^2	ω^2
0.965	0.947

5.3. ANOVA assumption check

Test	Statistic	p	Result
Shapiro-Wilk	0.91	0.059	Not significant (normality not rejected)
Levene's test	0.13	0.990	Not significant (homogeneity not rejected)

5.4. ANOVA fit summary

n	df_resid	R^2 (OLS)
21	14	0.965

5.5. Representative residual plots (OLS Residuals): Q-Q plot, residuals vs fitted

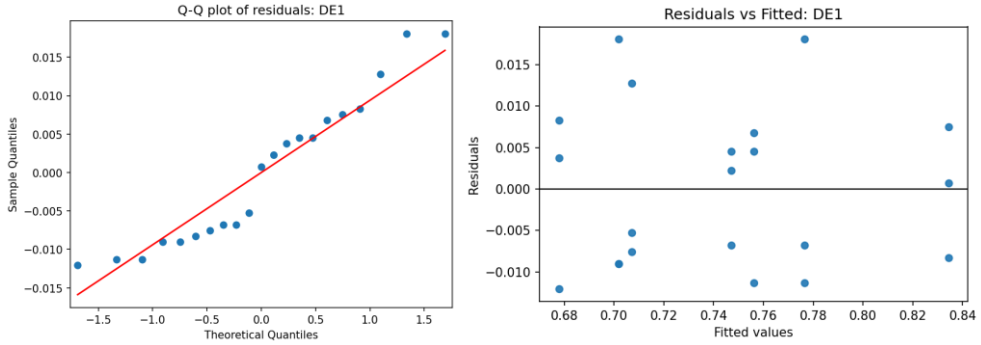

5.6. Dunnett's post-hoc test

Comparison (vs control)	ΔMean	95% CI (lower)	95% CI (upper)	Statistic	p	Result
Coarse GCC 5%	-0.06	-0.09	-0.03	-6.16	<0.001	Accepted
Coarse GCC 10%	-0.08	-0.11	-0.05	-8.33	<0.001	Accepted
Coarse GCC 15%	-0.13	-0.15	-0.10	-13.53	<0.001	Accepted
Coarse GCC 20%	-0.13	-0.16	-0.11	-14.09	<0.001	Accepted
Fine GCC 10%	-0.09	-0.11	-0.06	-9.29	<0.001	Accepted
Fine GCC 20%	-0.16	-0.18	-0.13	-16.65	<0.001	Accepted

6. $SEC_{forming}$

One-way ANOVA did not detect statistically significant differences among treatments, consistent with the near-flat response across dosage levels shown in Fig. 6. A moderate-to-low R^2 reflects that most of the total variance is not attributable to treatment level (i.e., weak signal relative to experimental scatter). Assumption checks did not indicate problematic departures from normality or homoscedasticity.

6.1. One-way ANOVA results

	Sum_sq	df	F	PR(>F)
Between (Treatment; 7 levels, incl. Control)	0.00	6	1.77	0.177
Residual	0.01	14	-	-

6.2. Effect-size reports

η^2	ω^2
0.431	0.180

6.3. ANOVA assumption check

Test	Statistic	p	Result
Shapiro-Wilk	0.94	0.258	Not significant (normality not rejected)
Levene's test	1.13	0.393	Not significant (homogeneity not rejected)

6.4. ANOVA fit summary

n	df_resid	R^2 (OLS)
21	14	0.431

6.5. Representative residual plots (OLS Residuals): Q-Q plot, residuals vs fitted

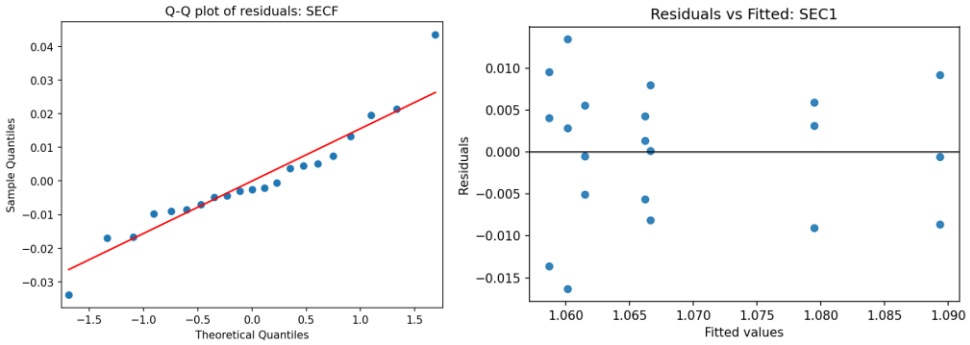

6.6. Dunnett's post-hoc test

Comparison (vs control)	ΔMean	95% CI (lower)	95% CI (upper)	Statistic	p	Result
Coarse GCC 5%	-0.01	-0.05	0.04	-0.41	0.996	Rejected
Coarse GCC 10%	0.02	-0.02	0.07	1.51	0.490	Rejected
Coarse GCC 15%	-0.01	-0.05	0.04	-0.38	0.998	Rejected
Coarse GCC 20%	0.01	-0.04	0.05	0.33	0.999	Rejected
Fine GCC 10%	0.02	-0.03	0.06	1.15	0.725	Rejected
Fine GCC 20%	0.03	-0.02	0.08	1.93	0.272	Rejected

7. $SEC_{HP\text{-}1min}$

71. One-way ANOVA results

	Sum_sq	df	F	PR(>F)
Between (Treatment; 7 levels, incl. Control)	0.00	6	4.28	0.012
Residual	0.00	14	-	-

7.2. Effect-size reports

η^2	ω^2
0.647	0.483

7.3. ANOVA assumption check

Test	Statistic	p	Result
Shapiro-Wilk	0.97	0.645	Not significant (normality not rejected)
Levene's test	0.40	0.866	Not significant (homogeneity not rejected)

7.4. ANOVA fit summary

n	df_resid	R^2 (OLS)
21	14	0.647

7.5. Representative residual plots (OLS Residuals): Q-Q plot, residuals vs. fitted

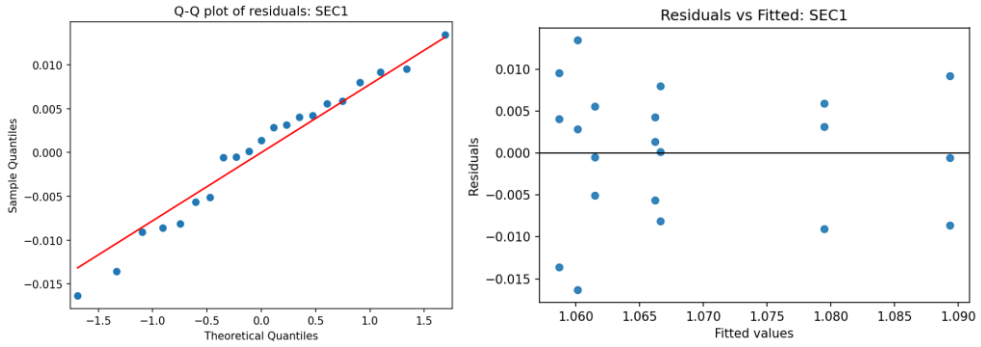

7.6. Dunnett's post-hoc test

Comparison (vs control)	ΔMean	95% CI (lower)	95% CI (upper)	Statistic	p	Result
Coarse GCC 5%	-0.03	-0.05	-0.01	-3.75	0.010	Accepted
Coarse GCC 10%	-0.03	-0.05	-0.01	-3.58	0.014	Accepted
Coarse GCC 15%	-0.02	-0.05	0.00	-2.92	0.050	Accepted
Coarse GCC 20%	-0.03	-0.05	-0.01	-3.94	0.007	Accepted
Fine GCC 10%	-0.02	-0.05	0.00	-2.97	0.045	Accepted
Fine GCC 20%	-0.01	-0.03	0.01	-1.27	0.648	Rejected

C. Polynomial fit summary for the representative cubic model (equal weights)

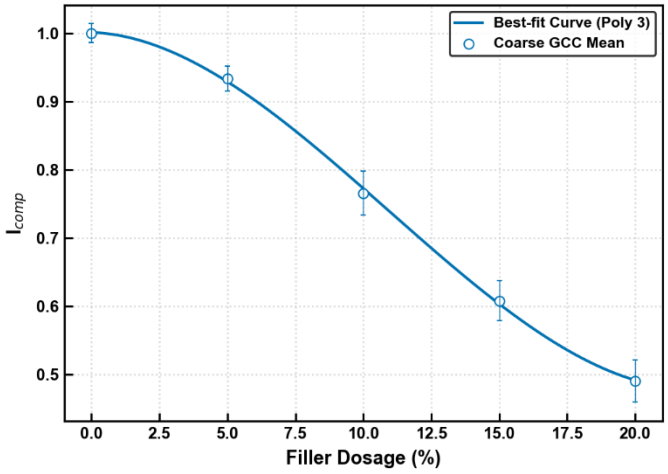

Model	n	df_resid	Adjusted R^2	RMSE	AICc
poly3	25	21	0.983	0.024	-177.176